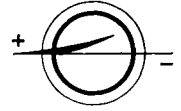


Electrophoresis '79
Advanced Methods
Biochemical and Clinical Applications



Electrophoresis '79

Advanced Methods
Biochemical and Clinical Applications

Proceedings of the Second International
Conference on Electrophoresis
Munich, Germany, October 15–17, 1979

Editor
Bertold J. Radola



Walter de Gruyter · Berlin · New York 1980

Editor

Prof. Dr. Bertold J. Radola
Institut für Lebensmitteltechnologie
und Analytische Chemie
Technische Universität München
D-8050 Freising-Weihenstephan
Federal Republic of Germany

CIP-Kurztitelaufnahme der Deutschen Bibliothek

[Electrophoresis seventy-nine]

Electrophoresis '79: advanced methods, biochem. and clin. applications; proceedings of the 2. Internat. Conference on Electrophoresis, Munich, Germany, October 15–17, 1979/ed. Bertold J. Radola. – Berlin, New York: de Gruyter, 1980.

ISBN 3-11-008154-7

NE: Radola, Bertold J. [Hrsg.]; International Conference on Electrophoresis <02, 1979, München>

Library of Congress Cataloging in Publication Data

International Conference on Elektrophoresis, 2d,
Munich, 1979.

Electrophoresis '79.

Includes index.

1. Electrophoresis-Congresses. 2. Isoelectric Focusing-Congresses.
3. Biological Chemistry-Technique-Congresses. 4. Chemistry Clinical-
Technique-Congresses. 1. Radola, B.J., 1931-

QP 519.9.E. 434 | 57 1979 574.19'28 80-13830

ISBN 3-11-008154-7

© Copyright 1980 by Walter de Gruyter & Co., Berlin 30. All rights reserved, including those of translation into foreign languages. No part of this book may be reproduced in any form – by photoprint, microfilm, or any other means – nor transmitted nor translated into a machine language without written permission from the publisher. Printing: Color-Druck, Berlin. – Binding: Lüderitz & Bauer, Buchgewerbe GmbH. Printed in Germany.

PREFACE

The International Conference "Electrophoresis '79" was held at the Technical University in Munich on October 15 - 17, 1979. It was the second of a projected series of international meetings organized with the objective to stimulate communication, information exchange and advancement of knowledge in all areas of electrophoresis. The need for this type of conferences is just an inference of a development in the field of electrophoretic methodology. In recent years not only have different techniques emerged but some have fused to powerful combinations, and it therefore seems justified to deal with different aspects of electrophoresis under a broader heading.

The conference in Munich was the largest of all electrophoretic meetings so far held. Much of the success of "Electrophoresis '79" has been achieved because it attracted most of the recognized leaders in the field. The conference was attended by participants from all parts of the world and from a broad range of academic disciplines. The format of the conference as well as the balanced representation from laboratories involved in the development and the application of electrophoresis has led to excellent personal interaction and much intellectual stimulation and benefit to the participants. The conference was certainly successful.

This volume contains a large portion of the papers presented either as oral reports or as posters at "Electrophoresis '79". The manuscripts have been compiled in four sections entitled: I. Theory and Methods, II. High Resolution Two-Dimensional Electrophoresis, III. Preparative Separations and IV. Biomedical and Biological Applications. These sections correspond to the major topics on which emphasis was placed at the conference. Not every manuscript fits precisely into one or another of the four sections but the most appropriate assignment has been made

VI

wherever possible. This volume could be produced because most authors were cooperative and admirably disciplined with regard to the deadline set for the submission of manuscripts. I take pleasure in expressing my appreciations and thanks to all contributors. The electrophoretic community owes much to them. I also greatly appreciate the efforts of the staff of Walter de Gruyter, Berlin, which led to the rapid publication of this volume.

Freising-Weihenstephan

Bertold J. Radola

ACKNOWLEDGEMENTS

I would like to acknowledge the splendid help of my laboratory staff in organizing the conference. I am indebted to Helga Piontek for excellent typing. I also thank my wife for volunteering her time and talent in helping to organize the conference and to prepare this volume for publication.

Financial help for the conference was provided by: Bio-Rad Laboratories, München; Desaga, Heidelberg; Deutsche Pharmacia, Freiburg; Immuno Diagnostika, Heidelberg; LKB Instrument, Gräfelfing; Serva Feinbiochemica, Heidelberg; Shandon Labor-technik, Frankfurt; Shimadzu (Europa), Düsseldorf.

CONTENTS

SECTION I, THEORY AND METHODS

GEL ELECTROFOCUSING WITH INCREASED DEGREES OF FREEDOM A. Chrambach, L. Hjelmeland and N. Y. Nguyen	3
pH-MOBILITY CURVES OF PROTEINS BY ISOELECTRIC FOCUSING COMBINED WITH ELECTROPHORESIS AT RIGHT ANGLES P. G. Righetti and E. Gianazza	23
PARTITIONING AND ELECTROPHORESIS IN FLEXIBLE POLYMER NETWORKS H. J. Bode	39
DOUBLE ONE-DIMENSIONAL SLAB-GEL ELECTROPHORESIS K. Altland and R. Hackler	53
ULTRATHIN-LAYER HORIZONTAL ELECTROPHORESIS, ISOELECTRIC FOCUSING, AND PROTEIN MAPPING IN POLYACRYLAMIDE GELS ON CELLOPHANE A. Görg, W. Postel and R. Westermeier	67
ULTRATHIN-LAYER ISOELECTRIC FOCUSING IN 50 - 100 μ m POLYACRYLAMIDE GELS ON SILANIZED GLASS PLATES OR POLY- ESTER FILMS B. J. Radola	79
ISOELECTRIC FOCUSING OF PROTEINS IN AGAROSE GELS AND DETECTION OF THE PROTEINS BY DIFFERENT STAINING PRO- CEDURES O. Vesterberg	95
AGAROSE ISOELECTRIC FOCUSING OF MONOCLONAL IgM AND IgG ANTIBODIES A. Rosén	105
IMMUNOPEROXIDASE STAINING AND RADIOIMMUNOBINDING OF HUMAN TUMOR MARKERS SEPARATED BY DIRECT TISSUE AGAROSE ISOELECTRIC FOCUSING C. A. Saravis, C. G. Cunningham, P. V. Marasco, R. B. Cook and N. Zamcheck	117

VIII

AGAROSE AS SUPPORTING MEDIUM FOR ANALYTICAL ISOELECTRIC FOCUSING: DETERMINATION OF THE RECENTLY DISCOVERED SUB-TYPES IN THE HUMAN SERUM PROTEIN Gc (GROUP SPECIFIC COMPONENT) M. Thymann	123
FACTS AND ARTEFACTS IN ISOELECTRIC FOCUSING E. Gianazza and P. G. Righetti	129
ISOELECTRIC FOCUSING PATTERNS OF SIMIAN VIRUS 40 (SV 40) TUMOR ANTIGEN: VARIOUS ALKYLATION PROCEDURES CAUSE REVERSIBLE ARTEFACTS K. Palme and R. Hanning	141
THE ROLE OF SIALIC ACID IN THE MICROHETEROGENEITY OF ALPHA ₁ ACID GLYCOPROTEIN: STUDY BY ISOELECTRIC FOCUSING AND TITRATION CURVES P. Arnaud, E. Gianazza, P. G. Righetti and H. H. Fudenberg	151
THE EFFECT OF ELECTRODE SOLUTIONS ON THE pH DRIFT IN THIN-LAYER ISOELECTRIC FOCUSING H. Delincée	165
QUANTITATIVE IMMUNOELECTROPHORESIS: A SURVEY AND SOME APPLICATIONS T. C. Bøg-Hansen, I. Lorenc-Kubis and O. J. Bjerrum	173
AFFINITY ELECTROPHORESIS: QUANTIFICATION AND CHARACTERIZATION OF GLYCOPROTEINS WITH LECTINS T. C. Bøg-Hansen	193
RECENT ADVANCES IN MICROELECTROPHORESIS V. Neuhoff	203
A SIMPLE, EFFECTIVE AND INEXPENSIVE EQUIPMENT FOR POLYACRYLAMIDE GEL ELECTROPHORESIS IN COOLED MICRO-CAPILLARIES R. Peter	219
LINEAR POLYACRYLAMIDE GRADIENT GELS FOR MOLECULAR WEIGHT ESTIMATION OF PROTEINS P. Lambin	227

SOLUBLE POLYACRYLAMIDE GRADIENT GELS IN THE SEPARATION AND ESTIMATION OF PROTEINS M. P. Brown and A. V. Emes	235
QUANTIFICATION OF PROTEINS SEPARATED BY TWO-DIMENSIONAL PAGE: A NOVEL DYE ELUTION TECHNIQUE COMPARED WITH A DENSITOMETRIC PROCEDURE O. H. W. Martini, J. Kruppa and R. Temkin	241
PREPARATION AND ANALYSIS OF PROTEINS AND PROTEIN FRAGMENTS BY TWO-DIMENSIONAL THIN-LAYER GEL FILTRATION AND ISOELECTRIC FOCUSING K. G. Welider	249
ENHANCEMENT OF LOAD CAPACITY IN ISOTACHOPHORESIS F. M. Everaerts, F. E. P. Mikkers and Th. P. E. M. Verhegen	255
A MODEL FOR THE USE OF MORE THAN ONE SINGLE BUFFERING COMMON COUNTERION IN ISOTACHOPHORESIS P. J. Svendsen and C. Schafer-Nielsen	265
SEPARATION OF MOLECULES IN STEADY STATE ELECTROPHORESIS SYSTEMS WITH ZONES CONTAINING MORE THAN ONE TERMINATING ION C. Schafer-Nielsen and P. J. Svendsen	275
FLOW-THROUGH CONTINUOUS THIN LAYER CARRIER-FREE ISOTACHOPHORESIS Z. Prusik, J. Štěpánek and V. Kašička	287
SECTION II, HIGH RESOLUTION TWO-DIMENSIONAL ELECTROPHORESIS	
TWO-DIMENSIONAL ELECTROPHORESIS: HIGH RESOLUTION OF PROTEINS AND AUTOMATIC EVALUATION OF THE PATTERNS UNDER DIFFERENT METHODOLOGICAL CONDITIONS J. Klose, J. Nowak and W. Kade	297
HIGH-RESOLUTION TWO-DIMENSIONAL ELECTROPHORETIC MAPPING OF HUMAN PROTEINS N. Anderson, J. J. Edwards, C. S. Giometti, K. E. Willard, S. L. Tollaksen, S. L. Nance, B. J. Hickman, J. Taylor, B. Coulter, A. Scandora and N. G. Anderson	313

X

ESTIMATION OF TWO-DIMENSIONAL ELECTROPHORETIC SPOT INTENSITIES AND POSITIONS BY MODELING J. Taylor, N. L. Anderson, B. P. Coulter, A. E. Scandora, Jr. and N. G. Anderson	329
INTERNAL CHARGE STANDARDIZATION FOR TWO-DIMENSIONAL ELECTROPHORESIS B. J. Hickman, N. L. Anderson, K. E. Willard and N. G. Anderson	341
A METHOD FOR STUDYING PROTEINS IN 2-D GELS USING THERMAL DENATURATION ANALYSIS S. L. Nance, B. J. Hickman, N. L. Anderson	351
THE QUANTITATION OF RADIOACTIVELY LABELED PROTEINS ON TWO-DIMENSIONAL GELS: TESTS OF A METHOD FOR ANALYZING CHANGES IN PROTEIN SYNTHESIS AND GENE EXPRESSION G. C. Stone, D. L. Wilson and G. W. Perry	361
TWO-DIMENSIONAL ELECTROPHORETIC MAPPING OF HUMAN ERYTHROCYTE PROTEINS J. J. Edwards, H. J. Hahn and N. G. Anderson	383
TWO-DIMENSIONAL ELECTROPHORESIS OF HUMAN SALIVA C. S. Giometti and N. G. Anderson	395
TWO-DIMENSIONAL ELECTROPHORESIS OF HUMAN URINARY PROTEINS IN HEALTH AND DISEASE S. L. Tollaksen and N. G. Anderson	405
ALTERATIONS OF TWO-DIMENSIONAL ELECTROPHORETIC MAPS IN HUMAN PERIPHERAL BLOOD LYMPHOCYTES INDUCED BY CONCAVALIN A K. E. Willard and N. L. Anderson	415
HIGH RESOLUTION TWO-DIMENSIONAL ELECTROPHORESIS (ISO-DALT) IN CLINICAL CHEMISTRY: COMPARISON WITH ROUTINE ELECTROPHORETIC AND IMMUNOLOGICAL METHODS A. K. Thorsrud, H. F. Haugen and E. Jellum	425
TWO-DIMENSIONAL MAPS OF HUMAN APOLIPOPROTEINS IN NORMAL AND DISEASED STATES V. I. Zannis and J. L. Breslow	437

ISOELECTRIC FOCUSING AND TWO-DIMENSIONAL ELECTROPHORESIS OF VIRAL PROTEINS AND VIRUS-INFECTED CELLS R. Drzeniek, C. Reichel, K. J. Wiegers, A. Hamann and M. Hilbrig	475
--	-----

SECTION III, PREPARATIVE SEPARATIONS

ISOELECTRIC FOCUSING, ISOELECTRIC POINTS, AND THE PREPARATIVE SEPARATION OF PROTEINS D. H. Leaback	493
PREPARATIVE MULTIPHASIC ZONE ELECTROPHORESIS AND ISOELECTRIC FOCUSING IN DENSITY GRADIENTS USING THE POLY-PREP N. Catsimpoolas, A. Stamatopoulou and A. L. Griffith	503
MULTIPHASIC COLUMN ELECTROFOCUSING: AN APPROACH TO COMPOSITE FRACTIONATION PROBLEMS D. Stathakos, A. Vellios and S. Koussoulakos	517
PREPARATIVE ELECTROFOCUSING OF ENZYMES INVOLVED IN AROMATIC DEGRADATION IN T. CUTANEUM A. B. Gaal and H. Y. Neujahr	529
PREPARATIVE FLAT-BED ISOELECTRIC FOCUSING OF LDH, MDH, ALD, SDH AND G-6.PDH FROM RABBIT LENS J. Bours, M. Garbers and O. Hockwin	539
CONTINUOUS-FLOW ISOELECTRIC FOCUSING OF PROTEINS P. Basset, J. Zwiller, C. Froissart, M. Recasens, R. Massarelli and G. Vincendon	545
RECYCLING OF CARRIER AMPHOLYTES BY ULTRAFILTRATION K. Goerth and B. J. Radola	555
REMOVAL OF SALTS AND CARRIER AMPHOLYTES FROM BILIPEPTIDES OF LOW MOLECULAR WEIGHT H.-P. Köst and E. Köst-Reyes	565
PREPARATIVE ELECTROPHORESIS IN GEL-BLOCKS WITH DISCONTINUOUS ELUTION H. Stegemann	571

XII

FURTHER DEVELOPMENTS IN PREPARATIVE DESPLACEMENT ELECTROPHORESIS IN GEL F. Hampson	583
VELOCITY GRADIENT STABILISED CONTINUOUS ELECTROPHORESIS A. R. Thomson, P. Mattock and G. F. Aitchison	591
PREPARATIVE DENSITY GRADIENT ELECTROPHORESIS OF LYMPHOID CELLS N. Catsimpoolas, A. L. Griffith, S. Gupta, R. A. Good and C. D. Platsoucas	607
PREPARATIVE CELL ELECTROPHORESIS IN A STATIC VERTICAL COLUMN STABILIZED WITH A HEAVY WATER GRADIENT C. J. van Oss and P. M. Bronson	623
SECTION IV, BIOMEDICAL AND BIOLOGICAL APPLICATIONS	
PAST, PRESENT AND FUTURE USES OF ELECTROPHORESIS IN CLINICAL MEDICINE R. C. Allen	631
TWO-DIMENSIONAL PROTEIN PATTERNS OF HUMAN BODY FLUIDS OBTAINED UNDER DISSOCIATING AND NON-DISSOCIATING CONDITIONS K. Felgenhauer	647
SIMPLIFIED DETERMINATION OF HEMOGLOBIN A _{1c} IN DIABETIC PATIENTS BY USE OF ELECTROFOCUSING J. O. Jeppson, B. Franzen and A. B. Gaal	655
A COMPARISON OF ISOELECTRIC FOCUSING AND ELECTRO- CHROMATOGRAPHY FOR THE SEPARATION AND QUANTIFICATION OF HEMOGLOBIN A _{1c} R. C. Allen, M. Stastny, D. Hallett and M. A. Simmons	663
INVESTIGATIONS OF HAEMOGLOBIN A _{1c} ANALOGUES BY ELECTROFOCUSING ON POLYACRYLAMIDE GELS C. J. Holloway, U. Schlanstedt-Jahn, I. Haeger, H.-J. Mitzkat and I. Trautschold	669

- ISOELECTRIC ENZYME PATTERN: A NEW CONCEPT FOR TUMOR CLASSIFICATION
H. J. Radzun, M. R. Parwaresch and D. Schmidt 679
- MONOCYTE-SPECIFIC ISOELECTRIC FOCUSING PATTERN OF LYSOSOMAL ACID ESTERASE: A NEW POSSIBILITY FOR CELL-SPECIFIC IMMUNOHISTOCHEMICAL IDENTIFICATION
J. W. Wittke, H. J. Radzun and M. R. Parwaresch 683
- ISOELECTRIC FOCUSING IN CELLULOSE ACETATE MEMBRANE AND FLAT-BED GRANULATED GEL: APPLICATION TO THE STUDY OF HUMAN ALDEHYDE DEHYDROGENASE ISOZYMES
S. Harada, D. P. Agarwal and H. W. Goedde 687
- CEREBROSPINAL FLUID (CSF) PROTEIN PATTERNS DETERMINED BY ISOELECTRIC FOCUSING IN MULTIPLE SCLEROSIS
B. Perthen and W. Müller-Beißenhirtz 695
- BINDING AFFINITIES BETWEEN VDBP AND VITAMIN D₃, 25-(OH)-D₃, 24-25-(OH)₂-D₃ and 1-25-(OH)₂-D₃ STUDIED BY ELECTROPHORETIC METHODS (PAGE-IEF, COMBINED IEF-ELECTROPHORESIS) AND PRINT-IMMUNOFIXATION
J. Constans, M. Viau, C. Gouaillard, C. Bouissou and A. Clerc 701
- IMMUNOFIXATION AFTER ELECTROFOCUSING: APPLICATION TO THE STUDY OF THE MICROHETEROGENEITY AND POLYMORPHISM OF SERUM PROTEINS
C. Chapuis-Cellier and A. Francina 711
- MICROHETEROGENEITY AND POLYMORPHISM OF THYROXINE-BINDING GLOBULIN: STUDY IN HUMAN SERUM BY RADIO-PRINT IMMUNOFIXATION
Y. Lasne, F. Lasne, O. Benzerara and P. Arnaud 727
- TWO-DIMENSIONAL IMMUNELECTROPHORESIS OF PLASMA-ANTITHROMBIN III IN THE PRESENCE OF HEPARIN-AGAROSE
H. Bleyl and H. Peichl 733
- DETERMINATION OF STREPTOKINASE ANTIBODY TITRE IN PLASMA OR SERUM BY AN IMMUNOELECTROPHORETIC METHOD
B. Skoog, A. Söderlindh and B. Granstrand 743

XIV

- TWO-DIMENSIONAL IMMUNOELECTROPHORESIS APPLIED TO THE SEMI-QUANTITATIVE DETERMINATION OF BENCE JONES PROTEIN IN PATHOLOGICAL URINES
M. Campens, A. Francina, H. Cloppet, C. Chapuis Cellier and P. Arnaud 753
- APPLICATION OF PHA IN ELECTROPHORETIC DIFFERENTIATION OF HUMORAL IMMUNOGLOBULINS
G. A. Spengler and R.-M. Weber 761
- FEASIBILITY OF STUDYING THE FUNCTIONAL NATURE OF HUMAN IgM SUBCLASS RESPONSES BY MEANS OF ANALYTICAL ISOTACHOPHORESIS
K. W. Hedlund, R. Wistar, Jr. and D. Nichelson 765
- IN VITRO INVESTIGATIONS OF THE GLUCURONIC ACID PATHWAY WITH THE AID OF ANALYTICAL CAPILLARY ISOTACHOPHORESIS
C. J. Holloway 775
- QUANTITATIVE RESOLUTION OF 1- AND 2-NAPHTHYL-GLUCURONIDES FROM SINGLE MIXED ZONES IN ISOTACHOPHROGRAMS
C. J. Holloway, S. Husmann-Holloway, G. Brunner, I. Trautschold and A. Baldesten 781
- A RAPID METHOD FOR QUANTITATIVE DETERMINATION OF URINARY OXALATE BY ANALYTICAL ISOTACHOPHORESIS
K. Schmidt and G. Bruchelt 791
- STUDIES ON SERUM CHOLINESTERASE ISOZYMES AND GENETIC VARIANTS IN HUMAN TISSUES USING POLYACRYLAMIDE GEL ELECTROPHORESIS
D. P. Agarwal, T. Münch, V. Stein and H. W. Goedde 797
- MATERNAL PLASMA PROTEIN VARIATIONS DURING NORMAL AND PATHOLOGIC PREGNANCY: A COMPARATIVE STUDY BY MEANS OF SDS-PAA ELECTROPHORESIS AND OSMOMETRIC EVALUATION OF NUMBER AVERAGE MOLECULAR WEIGHT
R. Schroeck and E. Feicht 805
- SERUM PROTEIN ANALYSIS BY MOLECULAR INTERPRETATION OF CELLULOSE ACETATE ELECTROPHORESIS: EVALUATION OF ITS CLINICAL USEFULNESS
F. Aguzzi, C. Petrini, G. Merlini, S. Perolini, F. Pozzi and S. D. Jayakar 811

GENETICAL AND BIOCHEMICAL CHARACTERIZATION OF A DOMINANT MUTATION OF MOUSE LACTATE DEHYDROGENASE W. Pretsch and D. Charles	817
VERTEBRATE MITOCHONDRIAL 55S RIBOSOMES: COMPARISON OF PROTEIN PATTERNS WITH BACTERIAL AND CYTOPLASMIC R-PROTEINS BY 2-D PAGE W. Czempiel and B. Ulbrich	825
ISOELECTRIC PEROXIDASE PATTERNS AS INDICATORS FOR GROWTH AND FOR THE EFFECT OF GROWTH REGULATORS IN TOBACO TISSUE CULTURES W. Rücker and J. Markotai	833
STUDY OF HEMOGLOBIN AND A SOLUBLE HEART PEROXIDASE IN LACERTA GALLOTI AND LACERTA STHELINI BY ISOELEC- TRIC FOCUSING Z. Gonzalez-Lama, R. H. Lopez Orge and A. M. Lamas	841
AUTHOR INDEX	847
SUBJECT INDEX	849

Section I

Theory and Methods

GEL ELECTROFOCUSING WITH INCREASED DEGREES OF FREEDOM

A. Chrambach, L. Hjelmeland and N. Y. Nguyen

National Institute of Child Health and Human Development, Bethesda,
MD 20205 USA

B. An der Lan

Bureau of Biologics, Food and Drug Administration, Bethesda, MD 20205 USA

Introduction

Electrofocusing started out as, and is widely applied as, a cookbook method of separation, which is controlled by the pI-ranges of the commercially available carrier ampholytes: Take one spoonful of such a preparation in the pI-range closest to your requirements, plus one spoonful of a "standard" polymerization mixture containing acrylamide, a pinch of Bis, a sprinkling of persulfate and a dash of TEMED, and bake for 30 min. Place it between strong acid and base, apply the protein, then an electric potential of 479.2 V, wait again for 2.3 h, stain-destain, or slice and measure pHs; count bands; publish the band pattern to demonstrate again history's most highly resolving method; publish the pI. End of recipe.

In this review of electrofocusing, we will take the opposite viewpoint. To us it appears axiomatic that, if one is aiming at optimal resolution, each separation problem requires its particular adaptation of a more general method. This review will deal, therefore, with ways to make electrofocusing more flexible, and to adapt it to particular separation problems. We will discuss flexible choice of apparatus, the various modes of "pH gradient engineering" and of stabilizing pH gradients, the choice of gel media, the detergents applicable to electrofocusing, the ways of circumventing conductance gaps, and of preparing proteins from each of the zones in analytical gel electrofocusing. With the ability to vary all these elements, electrofocusing becomes extremely adaptable to the specific

separation, and its resolving capacity is augmented.

1) Apparatus

If electrofocusing is to be used in a flexible manner, this must be reflected in the choice of apparatus. In other words, different types of apparatus are suited to different separation problems. If the object of experimentation is, for example, the measurement of pI, then the gel tube apparatus continues to excel, because of the ease with which protein positions and resolution, as well as pH gradients, can be monitored at variable electrofocusing times, and because of the load volume capacity, and of the economy of carrier constituents. When using cylindrical gels, pH gradients can be monitored semi-automatically with the commercially available pH gradient measuring device. Another advantage of tube apparatus, which could also be imparted to horizontal slab apparatus, are electrolyte chambers of sufficient capacity to prevent appreciable changes of anolyte and catholyte composition during the course of electrofocusing [(1) and for further discussion see below]. An important recent addition to the armory of gel tube electrofocusing equipment is a platinum wire attachment allowing voltages across the gel (excluding the reservoirs) to be monitored continuously during electrofocusing (Fig. 1). This is important when resistive uncharged anolytes and catholytes are used (see below). Another advance is a modification of a commercial electric gel slicing device (Fig. 2) capable of providing uniform slices of "non-restrictive" 6 %T, 15 %C_{DATD} gels (see below). If, on the other hand, electrofocusing kinetics and the rate of attainment of the steady-state are already known, and consequently electrofocusing time can be kept constant, horizontal slab apparatus offers the advantage that, at any one time of electrofocusing, direct comparisons of multiple band patterns within the same gel are possible (2). Furthermore, there is greater freedom in the choice of matrix material, because the horizontal support eliminates problems of mechanical support and wall adherence (see below). A more detailed discussion of the relative merits and disadvantages of tube and slab apparatus can be found elsewhere (1).

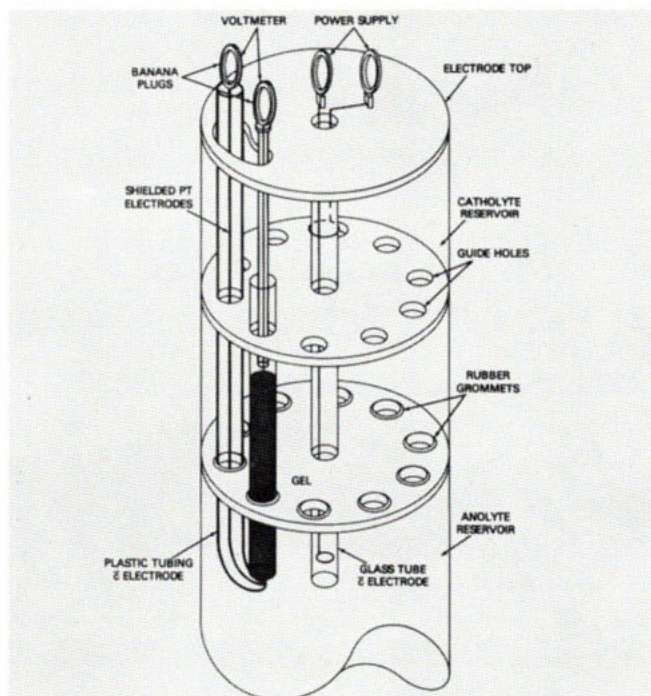


Fig. 1. Device for voltage measurement across the gel in gel electrofocusing with weakly acidic/basic or amphoteric analyte and catholyte at a pH at which their net charge approximates zero.

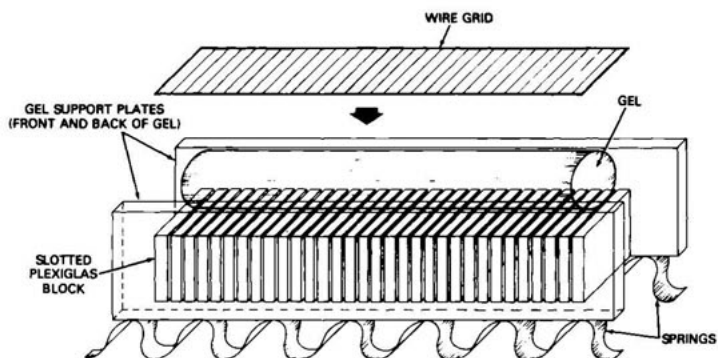


Fig. 2. Modification of an electric gel slicer (Hoefer Instruments, San Francisco) to facilitate cutting of "non-restrictive" 6 %T, 15 %C^{DADT} gels in electrofocusing. The cutting wires pass through the gel into grooves.

2) pH-Gradient Engineering

The proposition that the flatter the pH gradient around the steady-state pI-positions of the proteins, the better the resolution, appears self-evident. This concept appears to hold for separation, but is not supported by the available evidence for resolution. However, present data are still limited to 2 protein systems (3). Here it is important to distinguish between resolution and separation. Separations of either isohormones of human growth hormone or BSA and ovalbumin have been compared on either flat or steep pH gradients (Fig. 3). Although these data are too sparse to make generalizations, they allow us to define some of the conditions under which "the flatter, the better" holds. Fig. 3 shows that, although resolution (defined as $R = \text{peak separation} / \text{average standard deviation of each peak}$) is not enhanced on a flat pH gradient, separation is greatly improved, and preparative separation by a practical slicing method becomes possible. The price of improved separation, however, is that the average mobility of proteins is decreased. Hence, to reach their steady-state, longer electrofocusing times are required than are necessary using steeper gradients. This requirement is illustrated by Fig.6(3) where the pH values associated with the peaks of BSA and ovalbumin after 24 h of electrofocusing do not correspond to their pI' values, whereas after 48 h they do. The separation is better at 48 h, presumably because the steady-state has been reached. In view of the increased electrofocusing time, stabilization is a sine qua non for flat pH gradients. Fortunately, flatter pH gradients tend to be more stable than steeper ones (see below). A second and related problem concerns the rate of migration of the protein into the gel. Human growth hormone, for example, does not enter into flat pH-gradients unless it is first charged by dissolving in 0.1 M arginine (pH 10.5). Thus, it appears that the protein is titrated to a lower pH by the pH gradient sufficiently slowly to be able to maintain adequate mobility in penetrating the gel at a practical rate.

How does one go about making a flat pH gradient? There are three ways of tailoring pH gradients to the pH-range which circumscribes, as narrowly as possible, the pI's of the proteins that one wants to separate:

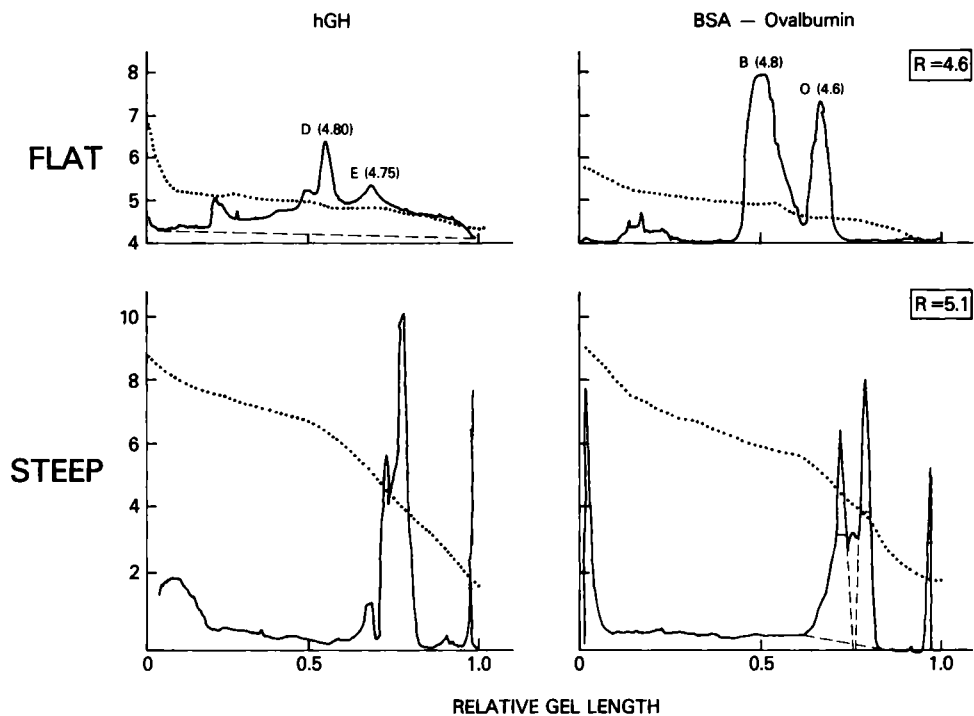


Fig. 3. Separation and resolution between isohormones of human growth hormone (hGH) and between BSA and ovalbumin: A comparison between flat and steep pH gradients. Gel concentration: 5 %T, 15 % C_{DATD} . Flat pH gradients: Ampholine (pI-range 4.5-5.0), threonine (pH 5.6) catholyte, diiodotyrosine (pH 4.4) anolyte. Electrofocusing time 48, 50 h respectively. Steep pH gradients: Ampholine (pI-range 3.5-10), 0.2 N KOH catholyte, 0.2 N H_2SO_4 anolyte. Electrofocusing time: 10 h. Resolution, R, is defined as the distance between peaks/average standard deviation of the two peaks. Data of ref. (3).

- A) Choice of carrier constituents². B) Constituent displacement.
C) Selection of anolyte pH.

A) Mixtures of simple buffer have been used as carrier constituents to make natural pH gradients in a particular pH-range; this is known as "buffer electrofocusing" of proteins (4). As one would expect, the addition of acidic carrier constituents to the mixture causes a shift of the pH gradient in the acidic direction, and of basic constituents a shift in the basic direction (Fig. 4) (3). Also, a single constituent, added

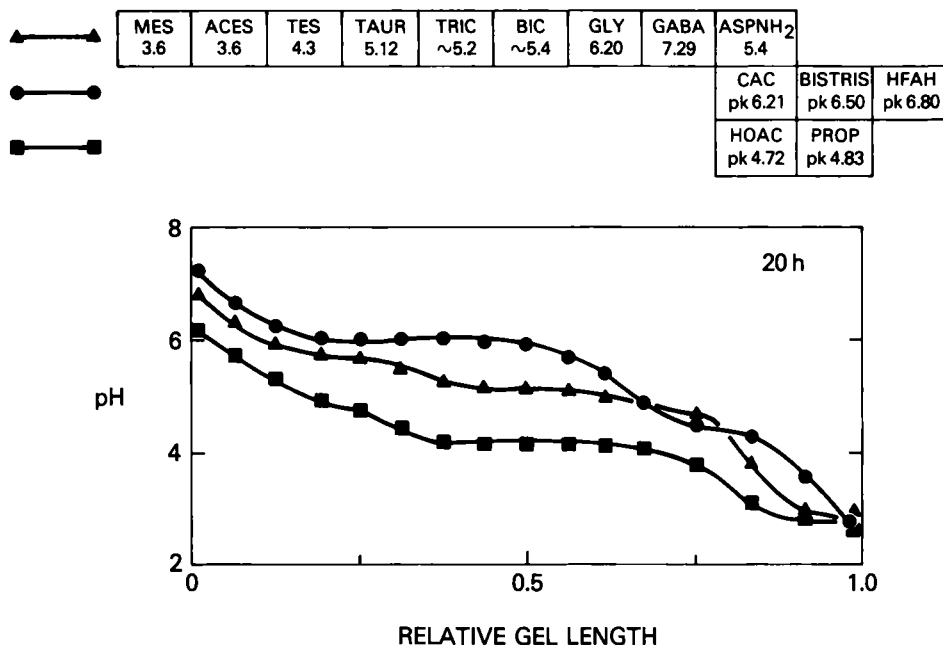


Fig. 4. Selection of specific carrier constituents in buffer electrofocusing. A common carrier constituent mixture of 8 amphoteric buffers was modified by adding basic (●—●), neutral (▲—▲) and acidic (■—■) constituents. Gel concentration and electrolytes as in Fig. 3. Data of ref. (3).

²Since natural pH gradients can be formed by mixtures of non-amphoteric buffers alone (4), we prefer the term "carrier constituent" to "carrier ampholyte."

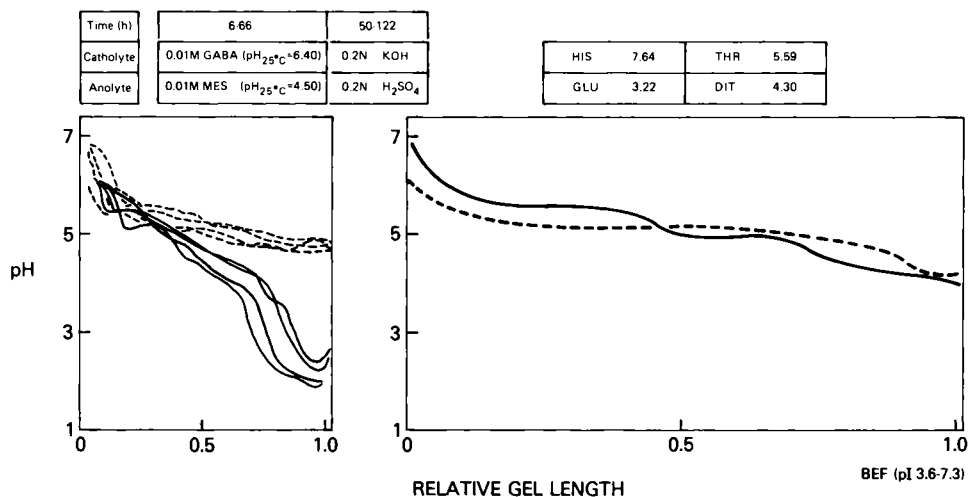


Fig. 5. pH Gradient design by constituent displacement. Buffer electrofocusing (pI-range 3.6-7.3). Gel concentration 5 %T, 15 % C_{DATD} . Left panel: Strongly vs. weakly acidic and basic anolyte and catholyte. Right panel: Fine adjustment of pH gradients, using terminal carrier constituents as the anolyte and catholyte. Data of ref. (23).

in large amounts compared to the concentrations of the other constituents, must flatten the pH gradient in the vicinity of its steady-state position (5). Thus, the addition of "separators" to multicomponent synthetic mixtures of carrier ampholytes also falls into this category of pH gradient design (5).

B) The pH-range of a gradient formed with either synthetic multicomponent mixtures of carrier constituents of the Ampholine type, or with buffers (4), can be narrowed by suitable choice of anolyte and catholyte (Fig. 5). For this purpose, the pH of anolyte and catholyte are chosen so that they are within the pH-range of the gradient, and so that they correspond to the desired terminal pH values of the gradient (6-8). Since anolytes and catholytes at suitable pH values cause displacement from the gel of all carrier constituents whose steady-state pH is less than the pH of the anolyte, or higher than the pH of the catholyte, this method of delimiting the pH gradient has been termed "constituent displacement." The success of "constituent displacement" depends on constancy of electrolyte pH with

time and thus requires relatively large (500-2,000 ml) electrolyte reservoirs [Fig. 13 of (9)]. In this regard soaked filter paper strips do not suffice as electrolyte reservoirs (10). For the same reason, i.e., maintaining a constant pH in the electrolyte reservoirs, it is advantageous to use amphoteric anolytes and catholytes (e.g., aminoacids) at their pI; when using fully deprotonated bases or fully protonated acids, catholyte and anolyte may have to be renewed once electrolysis causes significant pH changes.

C) It is possible to shift the pH gradient along the pH axis by varying the pH of the anolyte in a range outside the steady-state pH-range of the gradient (Fig. 6). Thus, the more acid the anolyte, the more acidic the pH gradient; the more closely the anolyte pH approximates the steady-state anodic terminal pH of the gradient, the more the pH gradient shifts in the cathodic direction (11). The stability of the gradient is also enhanced as the pH of the anolyte approaches that of the anodic terminus of the gradient [(11) and see below]. Anolyte control over the pH gradient primarily depends on the pH, rather than on the nature of the anion; progressive acidification of pH gradients with increasing concentration of phosphoric acid is evidence for this (12). However, the ability of the anolyte to control the pH gradient appears also to depend on its buffering capacity. Thus, weak acid anolytes (e.g., carboxylic acids) and strongly acidic anolytes with buffering capacity (e.g., phosphoric acid) exhibit this effect, whereas it is impossible to demonstrate a systematic shift of pH gradients as a function of pH with various concentrations of sulfuric acid, probably because the gradients are relatively unstable. In all experiments to date the catholyte failed to influence the pH gradient. It is important to note, however, that the catholyte was a relatively weak base, i.e., either histidine, lysine or arginine, or amines with pKs ranging from 6.8 to 8.1, when carboxylic acids [pKs (25°C) 3.7 to 6.2] or phosphoric acid were used as anolyte. It is still possible that the opposite effect may occur, when a strongly basic catholyte is combined with a weakly acidic anolyte, i.e., the catholyte may be used to induce an anodic pH gradient shift, whose extent depends on the alkalinity of the catholyte.

This expectation is supported by the fact that, under just these conditions (11), the pH gradient drifted toward the anode, rather than the cathode.

3) pH Gradient Stability

Although most users of gel electrofocusing will concede that pH gradient stability is a function of electrofocusing time and voltage, they would deny that this is of any consequence within the relatively short times allegedly required for protein separations. We take the opposite position

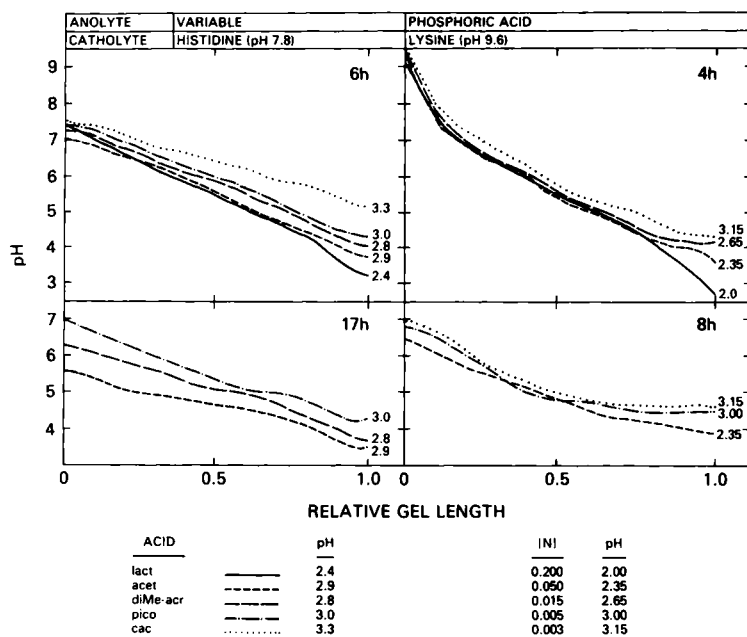


Fig. 6. Systematic shift of pH gradients as a function of the pH of the anolyte. Gel concentration: 6 %T, 15 %C_{DATD}. Ampholine pI-range 4-8. Catholyte: 0.1 M lysine. Left panel: Weakly acidic anolytes of varying pK. Right panel: H₃PO₄ at varying concentrations (11, 12).

on the following grounds: a) The plot of pH vs. electrofocusing time shows [e.g., (14-16)] that proteins in so-called "non-restrictive" gels attain a constant pH, i.e., an apparent pI (pI'), after a time that is roughly one order of magnitude greater than that required for the formation of the pH gradient (Fig. 7). In the representative cases shown the pI' was attained after 10 - 20 h of focusing at about 20 V/cm of gel and at 0-4°C, while the gradients formed after 2 - 3 h (17). b) When a protein occurs in multiple aggregation states (as most proteins probably do), it may take 80 h of electrofocusing [under the conditions described in Fig. 1 of ref. (18)] for protein patterns to condense and become uniform. c) The rate of migration, at a given voltage, is specific for each protein system and depends on the charge on the protein and on the degree to which it is retarded by the support medium. Those proteins with flat titration curves must, in addition, approach their isoelectric positions more slowly than those with relatively steep titration curves, as "poor and good carrier ampholytes" do respectively (19). All proteins approach true pI-positions on the pH gradient asymptotically. d) A further impediment to migration of proteins is the progressive appearance of conductance gaps (see below) which arise in the neutral pH-range at approximately one-third of the rate, at which the pH gradient forms (20). Thus, it appears necessary in each particular application of gel electrofocusing to stabilize the pH gradient for a time period sufficient for the attainment of the isoelectric endpoint (i.e., the position on the pH gradient where $pH = pI'$) under the chosen conditions of gel concentration, voltage and temperature. Such stabilization can be brought about, or at least enhanced, by the following measures: a) Flattening pH-range gradients (3, 21, 22) as demonstrated by comparing the degree of stability with that of wide pH gradients (3). b) Replacing the conventional strongly acidic anolyte and strongly basic catholyte by those constituting the steady-state anodic and cathodic terminals of the gradient (3, 21, 22). c) Approximating the anolyte pH to the steady-state anodic terminal pH of the pH gradient (11). d) Increasing the concentration of anolyte and catholyte (23). e) Increasing the carrier constituent concentration, although the time required to form the gradient is increased proportionately [Fig. 1 of (24)]. f) Increasing the viscosity (sucrose, urea) of the gel (2, 25), although apparently this is not effective in all cases

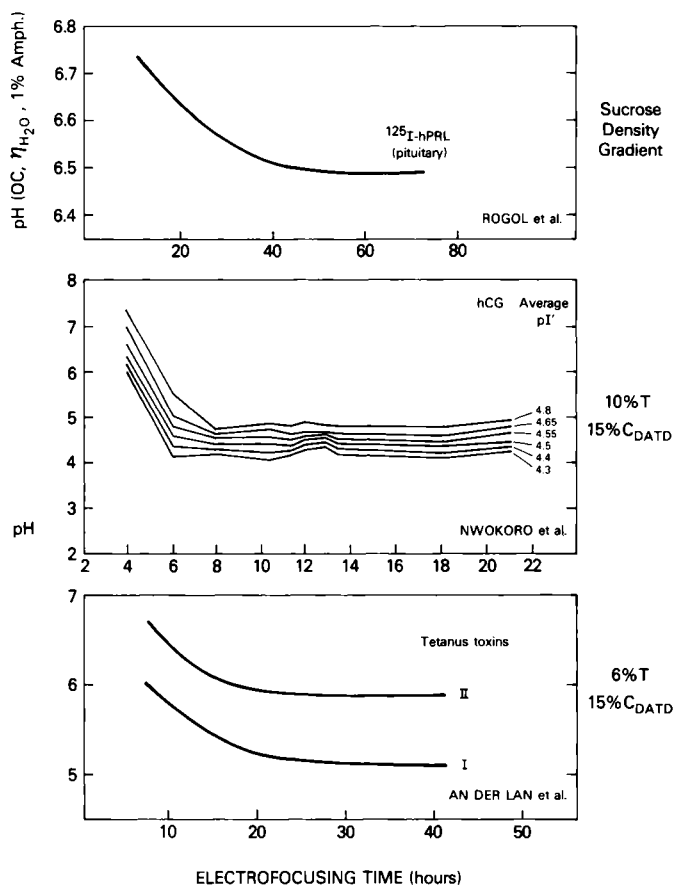


Fig. 7. Asymptotic approach of proteins towards their pI-positions in electrofocusing. Top panel: Radioiodinated human prolactin in sucrose density gradient focusing. Ampholine pI-range 5-8 (14). Center panel: The 6 major isohormones of human chorionic gonadotropin in electrofocusing on polyacrylamide gel. Ampholine pI-range 2-6 (16). Bottom panel: Radioiodinated tetanus toxin, Ampholine pI-range 3.5-10 (15).

(17, 23). g) Improving the wall adherence of the gel (13, 26).

4) Choice of Gel Media

Since the protein approaches its pI-position slowly and since optimal resolution depends on attainment of the steady-state [see above and (3, 4)], it is imperative to provide an effectively "non-restrictive" pore size in electrofocusing. This is not easily defined. A previously adopted working definition was to designate a pore size "non-restrictive" when it enabled maximally charged proteins (at either low or high pH) to migrate within the same Stacking Limits as a tracking dye (27). In electrofocusing, where proteins are relatively less charged, this criterion proves to be inadequate, i.e., mobilities on so-called "non-restrictive" gels appear low compared with mobilities on such media as granulated gels.

A) Polyacrylamide as gel matrix has the unique property of enabling one to vary pore size continuously over a very wide range. However, a wide variety of pore sizes is irrelevant for electrofocusing which demands "non-restrictiveness," rather than a tight fitting molecular sieve (in contradistinction to polyacrylamide gel electrophoresis). The popular low (2 to 5) % Bis-crosslinked polyacrylamide gels, even at low concentration (3.5 to 5 %T), provide more restrictive gels than the highly (15-50) % crosslinked gels (1, 27, 28). Of the latter types, the ones crosslinked with DATD provide the best mechanical stability and wall adherence, especially when gel tubes are pre-coated with linear polyacrylamide (13, 27). [The good adherence properties ("stickiness") of allyl-crosslinked gels may be due to a low average chain length compared to methylene-crosslinked gels. Allyl groups react at a lower rate than vinyl groups, so that allyl-pools accumulate during polymerization, which gives rise to an uneven distribution of crosslinks along the length of the polymer and to chain termination (29, 30).] As the degree of crosslinking with Bis increases above 10%, gels become progressively less "restrictive" and could be used for electrofocusing, if they could be firmly attached to the surrounding glass walls. This has been achieved by covalently bonding gel to glass with the vinyl siliconating agent,

A-174 (Pharmacia). However, in the single case (5 %T, 30 %C_{BIS}) subjected to electrofocusing, the wall adherence was lost after 6 h under conditions, where a 5 %T, 15 %C_{DATD} gel proved perfectly stable (26).

B) Agarose has the advantage over polyacrylamide in providing enormous pore sizes (compounds of molecular weight 150×10^6 and above are excluded from a 1% gel), in not swelling differentially as the pH varies along the gradient, in ease of gelation and possibly of protein recovery. Agarose gels excel in the ease with which they can be sliced. Since they can be liquefied by heating, measurement of radioactivity does not present the problems of gel solubilization or elution from gel slices encountered with polyacrylamide gels. Agarose has the disadvantage, compared with polyacrylamide, of a residual bound sulfate concentration sufficient to give rise to electroendosmosis (31), and of not adhering to glass. However, both of these problems are manageable. The sulfate concentration in recent commercial preparations has been reduced to a level which decreases electroendosmosis to such a low value ($R_f = -0.005$ in the buffer system used for comparison), that it may be negligible in the practice of gel electrofocusing (32). Presumably, the manufacture of special carrier ampholyte preparations for electrofocusing on agarose relates to this electroendosmosis problem. The wall adhesion problem can be neglected if agarose is either used on horizontal slab apparatus, particularly with commercially available coated plates, to which agarose adheres, or in vertical tubes or slabs supported by a strong polyacrylamide plug (L. Hjelmeland, unpublished data).

C) Granulated gels: Granulated dextran (Sephadex, Ultrodex, etc.), granulated polyacrylamide-agarose copolymer (Ultrogel, Indubiose, etc.), granulated agarose gels (Sephacrose, etc.), and polyvinylchloride and acetate (Pevikon) mixed with dextran (33) can be used for electrofocusing on horizontal gel beds. Compared to non-granulated polyacrylamide gels, these materials excel in the ease of protein recovery and non-restrictiveness, providing suitable pore sizes are selected to exclude the protein. However, as anticonvective media, their efficiency is not as high as continuous gel media, thus giving rise to broader zones. Conventionally, granulated gels are used in a horizontal slab apparatus. Here the packing

of horizontal beds evenly and reproducibly, and maintaining a uniform field across all channels of the conventional, relatively large beds may present problems. Cylindrical columns of Sephadex, supported by a polyacrylamide plug, can be used for electrofocusing of one or a few samples in a conventional gel tube apparatus (34).

5) Electrofocusing in Detergents

Recently, electrofocusing has been applied to hydrophobic proteins. Previously, it had been limited to those rare cases where non-ionic detergents could disaggregate and solubilize the protein. Even in those rare cases, the very large micellar sizes of non-ionic detergents gave rise to complexes containing several different protein molecules, and thus to uninterpretable pI values (35). Non-ionic detergents had the further disadvantage that they appeared to associate with the relatively non-polar basic carrier ampholytes (36), thus interfering with the formation of natural pH gradients in the alkaline range. Ionic detergents, on the other hand, suffer from the disadvantage that they increase the current and Joule heat. Furthermore, anionic detergents prevent formation of basic pH gradients presumably by binding to the carrier ampholyte species of the opposite net charge, and shifting their positions or displacing them (37). Amphoteric detergents of the alkyl-sulfobetaine type (Calbiochem. Cat. No. 693015-693023) are suitable for electrofocusing, since their large $pI-pK_p$ values should allow them to condense across the entire pH gradient (37). However, in the absence of assays for these detergents, there is at present no direct evidence for their immobilization across the pH gradient. The spreading of the methyl sulfobetaine, TMAPS (see below), across the gradient can be viewed as indirect evidence that long chain alkyl sulfobetaine detergents will also behave in such a manner. Similarly, the assumption that the presence of amphoteric detergents does not affect the pH gradient has only been verified for TMAPS. Although it is unlikely that the polar headgroups of such detergents, which resemble each other chemically, will affect the gradient, non-polar tails may do so, e.g., by binding to basic carrier ampholytes (36). The claim that amphoteric detergents would not denature proved to be unjustified, since some protein activities were

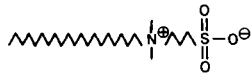
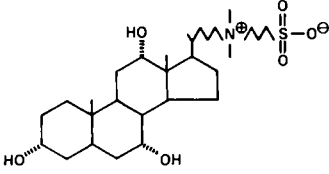
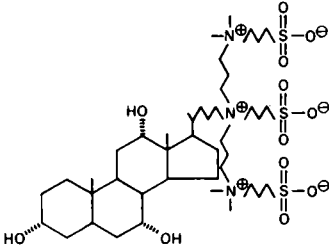
Zwitterionic Detergent	Solubility	Micellar Weight	Cytochrome P-450
	Soluble < 2°C	50,000	Denatured
	Insoluble	—	—
	Soluble	10,000	Native

Fig. 8. Structural characteristics of a non-denaturing amphoteric detergent suitable for electrofocusing. The flexible alkyl tail group of sulfobetaine-14 (SB14) renders this detergent denaturing to the hydrophobic membrane protein, cytochrome P-450 (37). In contrast, a rigid cholic-acid-like tail group makes the detergent non-denaturing. However, the relative insolubility of the molecule brought about by the rigid tail group needs to be compensated for by an increase in the polarity of the amphoteric polar head group of the detergent. (L. Hjelmeland, in preparation).

found to be destroyed (37). This defect has now been eliminated by replacing the flexible hydrocarbon chain of the amphoteric detergents with rigid cholic acid-type tails and by enhancing the polarity with multiple sulfobetaine polar head groups (Fig. 8). Such detergents are non-denaturing and suitable for gel electrofocusing (L. Hjelmeland, in preparation). Amphoteric detergents have the further advantage that micellar sizes are small compared with those of ionic detergents (40), thus ensuring that only a single copy of a protein, and particularly not several different proteins, can associate with (dissolve in) a single detergent

micelle (Fig. 8). Electrofocusing in detergents, however, still presents problems of protein fixation and staining, because detergents bind to dyes, and because they counteract the protein fixation required for staining. It is possible that this dilemma can be resolved by crosslinking the protein prior to staining, thereby protecting it from solubilization by the detergent, and by reducing the detergent concentration to below the critical micelle concentration, allowing for its rapid diffusion from the gel prior to staining.

6) Conductance Gaps

All natural pH gradients analyzed to date, whether generated with simple buffer mixtures or with synthetic carrier ampholytes, have developed conductance minima after some time of electrofocusing (20, 38). Claims of "even conductance" across pH gradients all rely on analysis at a single electrofocusing time prior, it is suspected, to the formation of voltage maxima in the neutral pH region [e.g. (39)]. Mechanistically, the formation of conductance gaps appears extraneous to the formation of natural pH gradients, since it has been observed in gels containing one amino acid only, and even when no carrier constituents were present at all (20). The conductance gaps (voltage maxima) develop after the pH gradient has formed and, in many cases, before the protein can reach its isoelectric pH on the pH gradient. Depending on the position of the protein relative to these voltage maxima (20) resolution may either be decreased by impeding the migration of the protein to its pI-position on the gradient or be enhanced (40). This problem can be overcome experimentally by conducting electrofocusing either in high (0.1 M) salt (19), or in the presence of an amphoteric "uncharged salt" of the trimethylamino-propionyl-sulfonate (TMAPS) type (40). Since 1 M TMAPS only conducts as well as 0.01 M KCl, it is not surprising that its ability to bridge conductance gaps is not sufficient to ensure that the gradient is permanently free of conductance gaps (40). But more highly conductive analogs of TMAPS with increased polarity have been synthesized and are expected to perform as "amphoteric KCl" in electrofocusing.

7) Preparative Gel Electrofocusing

The recovery of protein from non-granulated electrofocusing gel slices by diffusion is slow, and yields appear inversely related to the degree to which the isoelectric endpoint (and thus full resolution) has been attained (41). Presumably, this is due to the isoelectric precipitation of the protein in an efficiently anticonvective medium. (It is still open to question whether the granulated gel technique is similarly affected.) A solution to this problem has recently been developed. The procedure first deals with the problem of the isoelectric precipitation of the protein by applying either an alkaline Steady-State Stacking gel, or a quick exposure to alkali at 0°C, in order to charge the isoelectric protein. These conditions may, of course, denature active proteins. Further work is needed to determine whether detergent solubilization of the isoelectric protein with maintenance of activities is possible or preferable to exposure to an extreme of pH. After solubilization, the protein on electrofocusing gel slices can be extracted electrophoretically and concentrated by Steady-State Stacking (isotachopheresis) at any pH (18). An apparatus has been constructed which allows one to extract 10 slices, or pools of slices in any amount, simultaneously and in high yield (42). Since Steady-State Stacking is carried out on polyacrylamide, the concentrated protein fractions are contaminated by non-proteinaceous impurities derived from that medium. These are removed chromatographically prior to lyophilization. The overall yield of human growth hormone, the protein applied in this study, was 70%. The concentration step alone, tested on 10 and 100 mg loads of BSA per gel of 2.54 cm² surface area, yielded 80% (42). For electrofocusing separations on polyacrylamide gel, a protein load of 8 mg/zone/cm² appears tolerable; thus for most preparative purposes in biochemistry, the method applied to a single cylindrical electrofocusing gel of wide diameter (18 mm or less) yields the required milligram amounts of protein. Further application of this preparative gel electrofocusing method to multiple zones simultaneously will require development of a wide-diameter slab with even field strength across its length, and a guidestrip and horizontal gel slicing device designed to translate migration distances on a fixed and stained guidestrip to the original zone migration distances. Alternatively, protein detection on the entire prepara-

tive slab may be possible without need for a guidestrip, using as a detection tool the natural fluorescence of proteins at very low temperatures (43).

Among the preparative gel electrofocusing techniques applicable to granular gels, the continuous method of Fawcett (44) remains promising as a tool for preparing gram amounts. Progress has recently been made on the auxiliary techniques of carrier ampholyte recycling, continuous optical and conductance scanning by Bier, et al. (45). However, to make this approach widely applicable, ways must be found to maintain simplicity of operation and cost-effectiveness.

Conclusions

The possibility of engineering pH gradients to fit one's needs, the dynamics of pH gradients, the multiplicity of gel media and apparatus types, the application of amphoteric detergents, even conductance gaps can be turned to use in electrofocusing to improve protein separations. However, all of these devices remain empirical. A real control over electrofocusing must await a full physical-chemical understanding of pH gradient formation and decay, a prediction and computer simulation of its dynamics and its changes under the influence of the parameters with which this review has dealt. The recent analysis by Murel, et al. (46) may well signal the beginning of the necessary theoretical advance.

References

1. Chrambach, A.: J. Mol. Cell. Biol., in press (1979).¹
2. Righetti, P.G., Gianazza, E., Bosisio, A.B.: New Developments on Chromatography and Electrophoresis (Frigerio, A., ed.), Vol. 2, Elsevier North Holland, New York-Amsterdam, in press (1979).
3. Nguyen, N.Y., Chrambach, A.: J. Biochem. Biophys. Methods, submitted (1979).¹
4. Chrambach, A., Nguyen, N.Y.: Electrophoresis '78 (Catsimpoilas, N., ed.), Elsevier North Holland, New York-Amsterdam, pp. 3-18 (1978).¹

¹Available upon request.

5. Caspers, M.L., Posey, Y., Brown, R.K.: *Anal. Biochem.* 79, 166-180 (1977).
6. McCormick, A., Miles, L.E.M., Chrambach, A.: *Anal. Biochem.* 75, 314-324 (1976).
7. McCormick, A.G., Wachslight, H., Chrambach, A.: *Anal. Biochem.* 85, 209-218 (1978).
8. Chrambach, A., Nguyen, N.Y.: *Proc. International Workshop on Technology for Protein Separation and Improvement of Blood Plasma Fractionation* (Sandberg, H., ed.), Reston, VA, pp. 484-507 (1977).¹
9. Chrambach, A., Jovin, T.M., Svendsen, P.J., Rodbard, D.: *Methods of Protein Separation* (Catsimpoilas, N., ed.), Vol. 2, Plenum Press, New York, NY, pp. 27-144 (1976).¹
10. Arosio, P., Gianazza, E., Righetti, P.G.: *J. Chromatography* 166, 55-64 (1978).
11. An der Lan, B., Chrambach, A.: *J. Biochem. Biophys. Methods*, submitted (1979).¹
12. An der Lan, B., Chrambach, A.: *This Symposium*, Abstract No. 3 (1979).
13. Nguyen, N.Y., McCormick, A.G., Chrambach, A.: *Anal. Biochem.* 88, 186-195 (1978).
14. Rogol, A.D., Ben-David, M., Sheats, R., Rodbard, D., Chrambach, A.: *Endocrine Res. Comm.* 2, 379-402 (1975).
15. An der Lan, B., Habig, W.H., Hardegee, M.C., Chrambach, A.: *Arch. Biochem. Biophys.*, submitted (1979).¹
16. Nwokoro, N., Chen, C.-H., Chrambach, A.: *Endocrinology*, submitted (1979).¹
17. Baumann, G., Chrambach, A.: *Progress in Isoelectric Focusing and Isotachopheresis* (Righetti, P.G., ed.), Elsevier North Holland, New York-Amsterdam, pp. 13-23 (1975).
18. Nguyen, N.Y., Chrambach, A.: *J. Biochem. Biophys. Methods* 1, 171-187 (1979).
19. Righetti, P.G., Chrambach, A.: *Anal. Biochem.* 90, 633-643 (1978).
20. Jackiw, B.A., Brown, R.K.: *J. Biochem. Biophys. Methods*, submitted (1979).
21. Nguyen, N.Y., Chrambach, A.: *Anal. Biochem.* 82, 226-235 (1977).
22. Nguyen, N.Y., Chrambach, A.: *Anal. Biochem.* 82, 54-62 (1977).
23. Nguyen, N.Y., Chrambach, A.: *Anal. Biochem.* 79, 462-469 (1977).
24. Nguyen, N.Y., Chrambach, A.: *Anal. Biochem.*, 74, 145-153 (1976).
25. Doerr, P., Chrambach, A.: *Anal. Biochem.* 42, 96-107 (1971).
26. An der Lan, B., Nguyen, N.Y., Chrambach, A.: *Anal. Biochem.*, submitted (1979).¹
27. Baumann, G., Chrambach, A.: *Anal. Biochem.* 70, 32-38 (1976).

28. Rodbard, D., Levitov, C., Chrambach, A.: *Separation Sci.* 7, 705-723 (1972).
29. Tuszyński, G.P., Buck, C.A., Warren, L.: *Anal. Biochem.* 93, 329-408 (1979).
30. Schildknecht, C.E.: *Allyl Compounds and Their Polymers*, Wiley-Interscience, New York, NY, p. 14 (1973).
31. Ghosh, S., Moss, D.B.: *Anal. Biochem.* 62, 365-370 (1974).
32. Rosen, A., Ek, K., Aman, P.: *J. Immunol. Methods* 28, 1-10 (1979).
33. Otavsky, W.I., Bell, T., Saravis, C., Drysdale, J.W.: *Anal. Biochem.* 78, 302-307 (1977).
34. Jackiw, A.: *Abstr. XIth Internatl. Congr. Biochem.*, Toronto, p. 716 (1979).
35. Hjelmeland, L.M., Nebert, D.W., Chrambach, A.: *Electrophoresis '78* (Catsimpoilas, N., ed.), Elsevier North Holland, New York-Amsterdam, pp. 29-56 (1978).
36. Gianazza, E., Astorri, C., Righetti, P.G.: *J. Chromatography* 171, 161-169 (1979).
37. Hjelmeland, L.M., Nebert, D.W., Chrambach, A.: *Anal. Biochem.* 95, 201-208 (1979).
38. Jackiw, B.A., Chrambach, A.: *J. Biochem. Biophys. Methods*, submitted (1979).¹
39. Gelsema, W.J., De Ligny, C.L., Van der Veen, N.G.: *J. Chromatography* 173, 33-41 (1979).
40. Nguyen, N.Y., Hjelmeland, L.M., Chrambach, A.: *J. Chromatography*, submitted (1979).¹
41. Salokangas, A., Eppenberger, U., Chrambach, A.: *Biochim. Biophys. Acta*, submitted (1979).¹
42. Nguyen, N.Y., DiFonzo, J., Chrambach, A.: *Anal. Biochem.*, submitted (1979).¹
43. Mardian, J.K.W., Isenberg, I.: *Anal. Biochem.* 91, 1-12 (1978).
44. Fawcett, J.S.: *Ann. N.Y. Acad. Sci.* 209, 112-126 (1973).
45. Egen, N.B., Twitty, G.E., Bier, M.: *17th Ann. Aerospace Sci. Meet.*, New Orleans, LA, American Inst. Aeronautics and Astronautics, Publ., New York, NY, Doc. No. 79-0405 (1979).
46. Murel, A., Kirjanen, I., Kirret, O.: *J. Chromatography* 174, 1-11 (1979).

pH-MOBILITY CURVES OF PROTEINS BY ISOELECTRIC FOCUSING COMBINED WITH ELECTROPHORESIS AT RIGHT ANGLES

Pier Giorgio Righetti and Elisabetta Gianazza

Department of Biochemistry, University of Milano, Via Celoria 2, Milano 20133, Italy

Introduction

A direct knowledge of a given protein, and of its contaminants, titration curves would be a great strategic help for a biochemist attempting to purify it, since it would allow selection of the proper pH conditions for any subsequent purification work based on charge-dependent methods, such as electrophoresis, isotachopheresis, equilibrium isoelectric focusing (IEF) and ion-exchange chromatography. Unfortunately, only a handful of proteins have been titrated so far and only once they had been purified to homogeneity. In fact, in conventional potentiometric acid-base titrations, mixtures of different proteins would exhibit a single titration curve averaged over the amino acid compositions and the relative ratios of the various components in the mixture.

There are hints that things are rapidly changing. A major breakthrough came in 1976, at a meeting in Hamburg, when Rosengren *et al.* (1) presented "a simple method of choosing optimum pH conditions for electrophoresis", which was in fact a direct display in a polyacrylamide gel slab of the titration curves of all the proteins present in a mixture. This was achieved by a two dimensional technique by which the sample would move electrophoretically perpendicular to a pH gradient, generated by a stack of stationary carrier ampholytes. The sigmoidal, pH-mobility curves thus generated were indeed proportional to titration curves.

By further exploiting this idea, we have demonstrated the possibility of revealing the mutant charged amino acid in mutant phenotypes (2), of detecting liganded states of proteins (3) and of studying macromolecule-macromolecule

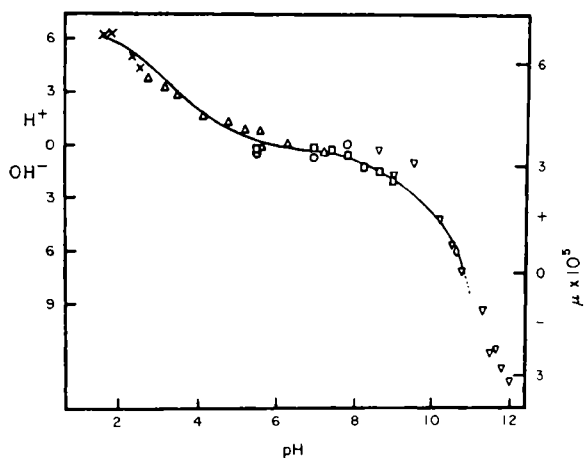


Fig. 1. Comparison of electrophoretic mobilities and dissociation curves of trypsin. Solid line: dissociation curve; points: electrophoretic mobilities in various buffers, ionic strength 0.13. X: NaCl-HCl; Δ , Na acetate-HCl; \square , CaCl_2 -barbiturate; \circ , MgCl_2 -barbiturate; ∇ , CaCl_2 -glycine; \diamond , CaCl_2 NH_4Cl (from Duke, J.A., Bier, M. and Nord, F.F.: Arch. Biochem. Biophys. 40, 424-430 (1952)).

interactions (4). Moreover, in the case of simple uni-uni-valent amphoteric molecules, we have derived an equation linking the electrophoretic mobility of the titrated ions with the pK' s of their anionic and cationic groups (5, 6). Thus, mobility data could be used to study protolytic equilibria of weak ionizable groups. In the present article we will review the results obtained so far and the possible future applications of this technique.

Historical

In the early fifties, attempts were made to correlate the electrophoretic mobility to protein charge, by using theories and equations derived by Smoluchowski (7), Debye and Hückel (8), Hückel (9) and Henry (10). The pH-mobility curves generated by electrophoresis at a series of different pH's in the pH 2-11 range were correlated to potentiometric titration data. In some cases, as shown in Fig. 1 for trypsin titration, a quite remarkable correlation among the two sets of data was achieved. However, generally,

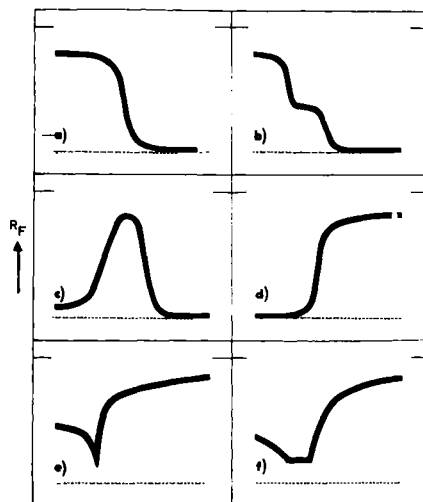


Fig. 2. Typical curve shapes obtained in thin layer chromatography perpendicular to a pH gradient. (a) monobasic acid; (b) dibasic acid; (c) amphoteric compounds, such as anthranilic acid; (d) monoacidic amine; (e) opium alkaloids; (f) tropane alkaloids (from Stahl (18); source: Elsevier Sci. Publ. Co.)

the electrophoretic charge was found to be lower than titration charge, possibly because the electrophoretic runs were performed at high ionic strength, up to 0.2. At these high values, part of the counter ions penetrate within the surface of shear of the protein, and by a steric effect diminish its electrophoretic charge. pH-mobility curves of even complex protein samples were run (11-13) as well as of different strains of viruses (14) and of intact, human red blood cells (15). In some cases alterations of the pH-mobility curves were exploited to study the combination of small ions with proteins, such as in the case of the binding of thiocyanate to insulin (16).

A completely different approach was used by Stahl (17, 18) who performed thin layer chromatography runs perpendicular to a pH gradient generated in the silica layer by diffusion of 0.1 N H_3PO_4 and 0.1 N KOH. As shown in Fig. 2 (and as visible in the beautiful color picture, Fig. 11 in ref. 17) the curves thus generated closely resemble direct titration curves. However, when we attempted to measure direct $\text{pK}'\text{s}$ from the inflection points of these curves, the results were a total failure. Thus (see Fig. 11 in ref. 17) the pK_{app} of methyl red should be slightly alkaline (above pH 7) and the

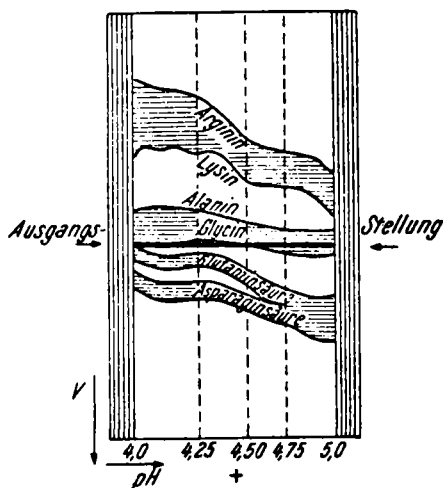


Fig. 3. pH-gradient electrophoresis of a mixture of Glu, Asp, Gly, Ala, Lys and Arg on a filter paper sheet. The pH gradient was created by diffusion of two solutions of acetic acid-pyridine buffered at pH 4 and pH 5, respectively. A voltage of 41 V/cm was applied for 20 min, perpendicular to the pH gradient (from Michl, ref. 19).

pK_{app} of neutral red should be slightly acidic (below pH 6.5) while in reality the reverse is true (see ahead). This means that the rate of migration of an ionic compound in thin layer chromatography is not solely a function of the degree of ionization of its ionizable groups, but depends also on other properties of the molecule (e. g. its polarity, hydrophobicity, etc.).

Michl (19) was the first to attempt to develop direct titration curves by electrophoresis perpendicular to a pH gradient generated on a filter paper. Fig. 3 shows the attempt to titrate a mixture of amino acids over a one pH unit gradient. Notice that, at least in the case of Glu and Asp, the experiment was successful since the two curves merge above pH 5, where the charge density on the two molecules becomes identical. That was the year 1952, and we feel it was really a pioneering approach, preceding even Kolin's work (20). Another German couple, Friedli and Schumaker (21), should be credited with having invented affinity-electrophoresis, which is the fashion of the 1980's. Oddly, no one seems to be aware of both works. We wonder if it could be due to the fact that most of their production has appeared in a strange, middle-European dialect, which we understand is called "German".

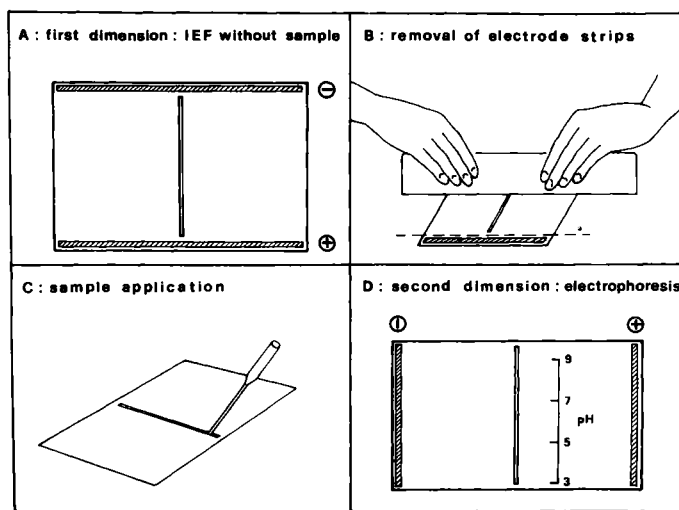


Fig. 4. Experimental procedure for generating titration curves by IEF-electrophoresis. The pH gradient is first formed by focusing the carrier ampholyte mixture (A); the electrode strips are then removed (B), the sample is applied in a trench cut perpendicular to the pH gradient (C) and the second dimension run is started perpendicular to the first dimension axis.

Methodology

Unfortunately, all these early attempts were plagued by having to perform a series of electrophoretic runs, at known, fixed pH's, or, when the pH was preformed on the support, by difficulties in charting it and by its marked instability in time. Our present technique is made possible by the fact that, in the second dimension, the pH remains stationary up to two hours of electrophoresis, thus allowing the generation of a smooth titration curve in the pH 3-10 range. Fig. 4 shows how our pH-mobility curves are developed. A 2 mm thick polyacrylamide gel slab is cast with a trench in the middle, 10 cm long, 1.5 mm deep and 1 mm wide, which can be loaded with up to 150 μ l sample. The first dimension consists in sorting electrophoretically the carrier ampholytes contained in the gel, thus generating a stationary pH gradient. No sample is applied at this stage. At this point, the electrode strips, with the respective gel layers underneath, are chopped away with a long butcher knife (Fig. 4B). This step is essential, otherwise a tremendous

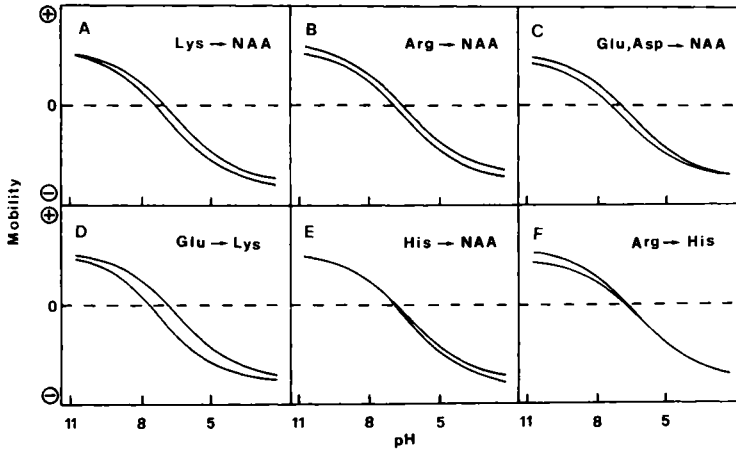


Fig. 5. Theoretical titration curves of hemoglobin and its genetic mutants in the presence of a given amino acid substitution. For further details, see text (from Righetti and Gianazza (6); source: Pergamon Press).

heat will be generated in these regions in the second dimension, due to the presence of 1 M acid and base. New electrodes are then applied perpendicular to the first run and the trench filled with the sample to be analyzed (Fig. 4C). Now, electrophoresis perpendicular to the stationary pH gradient is run, usually at 600 V over 12.5 cm and for periods of 10 up to 45 min (Fig. 4D).

Results

1) *Genetic mutants.* It is possible to perform "differential" titration curves by running a protein and its genetic mutants in a mixture. The shape of the respective titration curves should reveal which charged amino acid had been substituted in the mutant phenotype. Fig. 5 depicts theoretical "pH-mobility curves" calculated for a protein (in this case hemoglobin, Hb) and for some of the most common mutants on charged amino acids: Lys (5A), Arg (5B), Glu or Asp (5C) and His (5E) to neutral amino acid as well as double charge mutants (e. g. Lys → Glu, Fig. 5D) or same charge replacements (e. g. Arg → His mutations, Fig. 5F). While in all cases the mutation is directly inferred from the titration curve, in the case of Arg → neutral mutants the

information is only indirect, since it is almost impossible by present day IEF to obtain any stable pH gradient above pH 10.5. Therefore, within our titration range, the two curves will always be parallel and it will be impossible to distinguish, for instance, between an Arg \rightarrow neutral mutant at the alkaline extreme, from a protein and its phosphorylated derivative, at the acidic extreme. For this reason, we have limited our treatise to pure protein moieties, or to apoproteins in the case of conjugated proteins. Nevertheless, our data still apply to conjugated molecules, provided that no charge changes take place in the prosthetic group in going from the "wild type" to the mutant phenotype. An additional limit of the present technique is that, due to the quite close pK 's of β and γ carboxyls, it is difficult to differentiate between Asp and Glu mutants, when titrating in the wide (pH 3-10) range. However, by expanding the acid portion of the titration curve (e. g. by using a narrow, pH 2-5 range) it should be possible to distinguish a Glu from and Asp mutant, since in the former case the two titration curves should join at pH *ca.* 3.2, *i. e.* half a pH unit higher than the confluence point of Asp mutants. Within these boundaries, these theoretical titration curves were experimentally verified by running normal human adult hemoglobin (HbA) mixed with any of the following mutants: HbS, HbC, Hb Su-resnes and HbG Philadelphia (2).

2) *Macromolecule-ligand interaction.* Protein-ion interactions have usually been quite difficult to be demonstrated by any electrophoretic technique, since often the small bound ion is quickly removed upon application of the electric field, to an extent proportional to the square of the voltage applied (22). Moreover, if the complex is stable in a pH region removed from the pI of the free protein or of the complex species itself, equilibrium IEF will fail to reveal it, as there will be ample time for the ligated species to split apart during the transient state.

We have been able to run titration curves of met Hb-inositol hexaphosphate (IHP) and met Hb-inositol exasulphate (IHS) complexes. The pH ranges of stability of these liganded states are pH 4.5-6.0 for met Hb-IHP and pH 3.7-6.0 for met Hb-IHS. Both complexes appear to have an association constant (K_a) of the order of μM , and exist under our experimental conditions up to 8-10 min of electrophoresis. When the Hb-2,3-diphosphoglycerate complex (known

to have a K_a greater than mM) was titrated, only the titration curve of free Hb could be demonstrated within the pH 3-10 range, indicating that the complex was immediately split by the current. It should be possible, however, to detect very short lived intermediates by performing the experiment at -10° to -15°C . An example is given by the interaction between doxorubicin (an antimitotic used in tumor therapy) and human serum albumin (HSA). No complex could be detected when running the pH mobility curve at 4°C , however, at -10°C the ligated state could be observed up to 20 min of electrophoresis. Moreover, the complex existed only above pH 8.5, suggesting that the interacting species was the uncharged doxorubicin (deprotonated on the $3'$ - NH_2 group in the sugar ring) (unpublished experiments with M. Menozzi and C. Gelfi).

3) *Macromolecule-macromolecule interactions*. Interacting protein species were extensively studied in the fifties with the aid of the Tiselius apparatus, by taking advantage of the markedly non-enantiographic patterns in the ascending and descending limbs of the U-shaped cell. One of the most elegant physical studies of protein-protein interaction is the work of Singer's group (23-26) on the soluble complexes of protein antigens with the corresponding antibodies. We have taken advantage of our two-dimensional technique to study the interaction between cytochrome b_5 (Cyt b_5) and met Hb. While the two proteins, when run singly in the gel, develop the classical sigmoidal shape of a titrated macromolecule, when run in a mixture they exhibit strongly distorted patterns, above the pI in the case of Cyt b_5 and both, above and below the pI for met Hb. The maximum interaction appears to occur in the pH 8.0-8.3 range, and is consistent with a predominant role of Lys residues of met Hb in the binding to acidic amino acids of Cyt b_5 (4).

We have also studied the interaction between hemoglobin and haptoglobin (Hp), as well as the binding of intact α and β globin chains to Hp. While Hp-Hb complexes followed the well known patterns and stoichiometries reported in the literature (see Fig. 6) and were completely stable in the pH 3-10 range, indicating a predominant role of non-ionic interaction, free β chains did not appear to bind to Hp while free α globins exhibited an intriguing, pH-dependent pattern, indicating a mixed type of interaction (to be published with R. Krishnamoorthy, D. Labie and M. Waks).

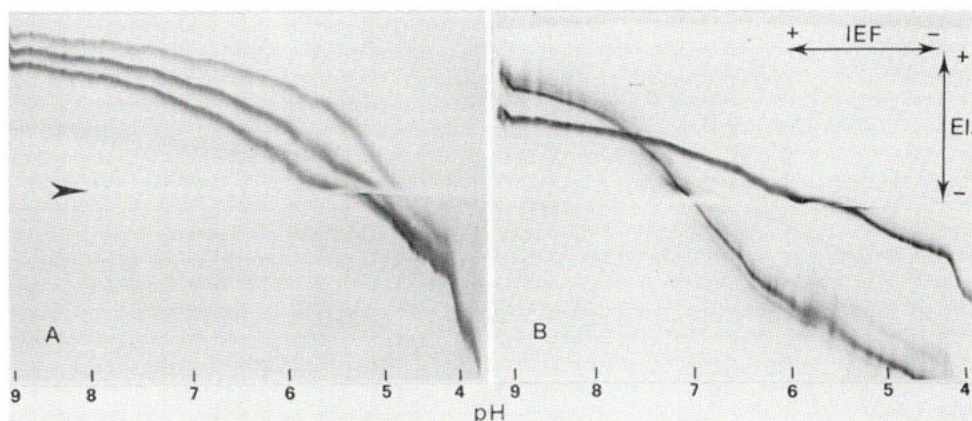


Fig. 6. Titration curves of Hp-Hb complexes in a 3:1 molar excess of Hp (A) and in a 3:1 molar excess of Hb (B). The three curves in A are: free, excess Hp (pI 4.5), Hp-Hb, 1:0.5 molar, complex (pI 5.0) and Hp-Hb, 1:1 molar, complex (pI 5.5). The two curves in B are: Hp-Hb, 1:1 molar, complex (pI 5.5) and excess free Hb (pI 7.0). The two arrows and positive and negative symbols represent the direction and polarity of isoelectric focusing (IEF) and electrophoresis (EI.). The arrowhead indicates the sample application zone (*i.e.* the zero-mobility or isoelectric plane) (R. Krishnamoorthy, P.G. Righetti, D. Labie and M. Waks, unpublished).

Generally speaking, if the protein-protein complex is strong enough, it can also be detected by conventional electrophoretic techniques, as a new peak arising in the electrophoretic pattern upon running the mixture, and usually exhibiting a mobility intermediate between that of the free species. This is in fact what has been found by Singer's group (23-26) by free boundary electrophoresis and, more recently, by Hedlund and Nicholson (27), working with soluble complexes of HSA antibodies with HSA itself, by isotachopheresis in a capillary tube. Both techniques, however, do not permit the study of the stability of the complex as a function of pH, information which is of utmost importance for an understanding of the mechanism of ionic interactions. This could be obtained, but only by running a series of different experiments at discrete pH intervals, a painstaking job. In capillary isotachopheresis, even though the run is performed in a pH gradient, there is no way, at present, to chart the pH course between the leading and terminating electrolytes. Moreover, in conventional electrophoretic techniques, the high ionic strength usually employed in the buffers (often 50 mM or higher) is

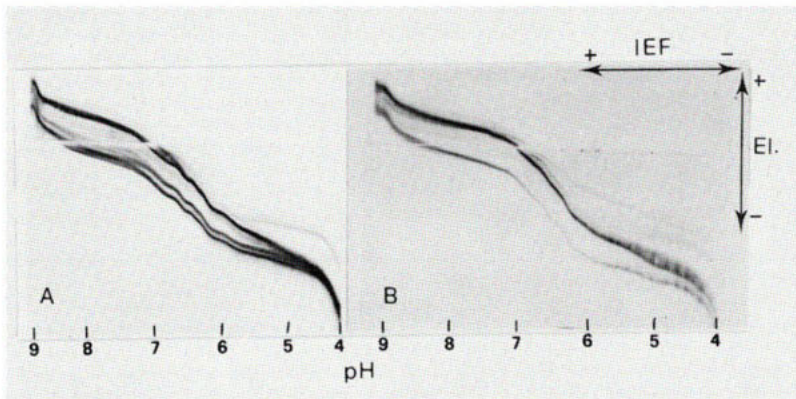


Fig. 7. Titration curves of reduced, alkylated and desalted, heme-free α - and β -globin chains in 8 M urea (A) and 8 M urea and 1% NP-40 (B). All other conditions and symbols as in Fig. 6. The pH gradient has been corrected for the presence of 8 M urea. Notice, in the presence of detergent (B), the absence of precipitation and splitting for each chain around its pI value (E. Gianazza and P.G. Righetti, unpublished).

enough to disrupt weakly interacting species. In the present technique, the average buffer molarity in the gel should be around 10 mM (in terms of each individual carrier ampholyte focused at its pI), thus allowing for a considerably longer half-life of the interacting macromolecules.

4) *Titration curves in 8M urea and detergents.* Since pH-mobility curves of macromolecules, under native conditions, do not allow direct titration of all ionizable groups, but only of surface groups accessible to solvent and of groups not engaged in subunit contacts, or other interactions, we have developed electrophoretic titrations in denaturing solvents, such as 8 M urea. In this system, many proteins will exist as random coils, subunits will be split apart, buried groups will be exposed to the solvent and the macromolecule will be stripped free of non-covalently bound ligands or co-factors. We have thus run titration curves of heme-free, α and β globin chains in 8 M urea (28). This system allows a "bird-eye view" of the total amino acid composition of these two chains. In fact, since α and β chains differ mostly in their acidic residues, they should come very close below pH 3, where only one positive charge difference is left. Disturbing features are encountered in the fact that they indeed join around pH 3 (while

they should not) and that each curve forks both, below and above the pI, probably due to partial precipitation and aggregation in the pI neighborhood. However, if the titration curves are performed in 8 M urea and 1% Nonidet P-40 (NP-40), both these disturbances disappear (see Fig. 7), since probably the detergent, by binding to hydrophobic stretches in the polypeptide chain, prevents inter-chain interactions, which would favor aggregation and flocculation in proximity of the isoelectric point.

5) *Titration curves in highly-porous matrices.* All the data presented so far do not allow direct measurement of absolute mobilities, as customary in free boundary electrophoresis, with the Tiselius unit. This is due to the sieving properties of the anticonvective medium (usually a 5 to 6% acrylamide gel), which hinders the migration of the titrated macroion to an extent proportional to its molecular weight. In order to overcome that, we have attempted to run titration curves in highly porous media (acrylamide gels containing 15 to 40% cross-linker, either N,N'-methylene bisacrylamide (Bis) or diallyltartardiamide (DATD))(29, 30) which should allow almost unhindered migration of macromolecules in the multimillion M.W. range. Unfortunately, highly cross-linked gels have been found to be poorly characterized support media (31). DATD gels contain up to 80-90% unpolymerized DATD which reacts with proteins and produces gluey and highly stretchable matrices. The conversion into polymer cannot be affected by time nor high temperatures, since DATD is an inhibitor of polymerization. On the other hand, highly cross-linked Bis gels, at 40 to 50% C levels, are too hydrophobic and produce a collapsed matrix which keeps exuding water. An acceptable compromise are 30% C_{Bis} gels, which are stable and allow unhindered migration of globular proteins up to 0.5 million daltons (31). We are now developing titration curves in 0.5 to 0.8% agarose EF, a very low electroosmosis brand of agarose introduced by LKB and compatible with IEF. This new support medium (which is cast and bound against an hydrophylic plastic sheet) is easily cast, stained, destained and dried.

6) *Direct pK determinations from titration curves.* The results presented so far have been only qualitative and semi-quantitative in nature. We have attempted to develop a mathematical theory which would allow direct pK determination of ionizable groups from the shape of the pH-mobility curves.

We have succeeded on that, but only with simple, uni- uni-valent amphoteric compounds. By assuming that:

- a) the total electrophoretic mobility (M_t) of a mono- mono-valent amphoteric molecule is proportional to its degree of ionization;
- b) the viscosity and degree of polymerization of acrylamide are constant along the gel length;
- c) the conductivity along each focused Ampholine species is constant;
- d) the molecule does not change size or shape along the pH 3-10 gradient (e.g. it does not aggregate with itself nor complexes with the carrier ampholytes), we have derived the following equation:

$$M_t = h \frac{10^{pK_c - pH} - 10^{pH - pK_a}}{1 + 10^{pK_c - pH} + 10^{pH - pK_a}} \quad (1)$$

where K_c and K_a are the dissociation constants of the cation and the anion, respectively, and h is a proportionality coefficient. This equation is easily verified by considering that, at the isoelectric point ($pH = pI$) the electrophoretic mobility is zero ($M_t = 0$) and therefore eq. (1) becomes:

$$pI = \frac{pK_c + pK_a}{2} \quad (2)$$

which is the well-known equation giving the isoelectric point as the arithmetical mean of the two pK 's of a mono- mono-valent ampholyte. A direct determination of either pK_c or pK_a can be made by measuring the pH ($pH_{\frac{1}{2}}$) corresponding to $\frac{1}{2}$ mobility in the cathodic or anodic directions, respectively, corrected by a factor accounting for the influence of the degree of ionization of the opposite-charge ion on the mobility curve of the ion being measured. For instance, in the case of doxorubicin (5), since only the cationic mobility can be measured within our titration range, by substituting in eq. (1) the value $pK_a = 2pI - pK_c$ and the value $pH_{\frac{1}{2}}$ corresponding to $\frac{1}{2}$ mobility, we obtain:

$$pK_c = pH_{\frac{1}{2}} - \log(1 - 3 \times 10^{-2(pI - pH_{\frac{1}{2}})})$$

A similar equation can be derived for pK_a measurements. Notice that, if the distance between the two pK 's (ΔpK) is greater than 1.5, the correction factor becomes negligible (it amounts to less than 0.02 pH units) and can

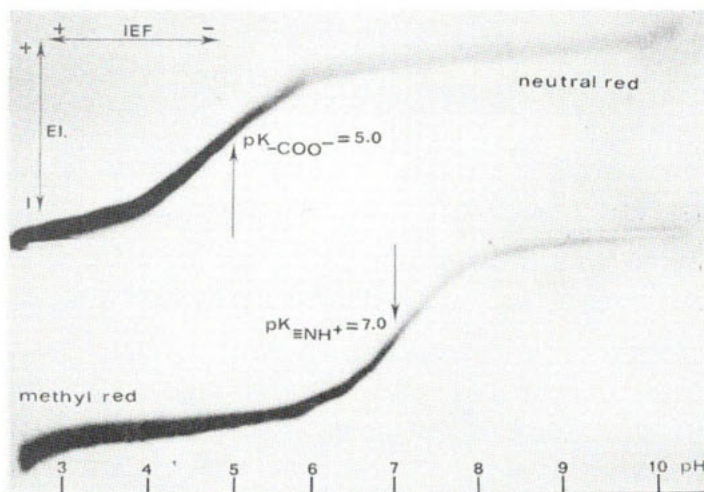


Fig. 8. Titration curves of neutral red and methyl red. The trench was filled with 150 μ l of a mixture of 20 μ g neutral red and 60 μ g methyl red, in 8M urea. The gel contained 6% acrylamide, 2% Ampholine pH 3-10 and 8M urea. The second dimension was run for 15 min at 12°C and 600 V/12.5 cm. The pH gradient has been corrected for the presence of 8M urea. All symbols as in Fig. 6 (E. Gianazza, C. Gelfi, L. Valentini and P.G. Righetti, unpublished).

be ignored. In this case, as well as in the case of simple, weak acids and bases, the pK_a or pK_c will simply be derived by measuring the pH of $\frac{1}{2}$ mobility. This case is illustrated in Fig. 8, which shows the titration curves of neutral red (an amphoteric molecule, with $\Delta pK = 2.5$) and methyl red (a simple, weak base). In both cases the pK has been derived as $pH_{\frac{1}{2}}$; both pK data were in excellent agreement with spectrophotometric titration values and in the gel could also be found by visual inspection as the pH of $\frac{1}{2}$ color change (from bright violet in the acidic region to faint orange in the basic region) (to be published with L. Valentini and C. Gelfi). As previously stated, the "true" pK values we have measured here are just the reverse of what could be roughly estimated from chromatographic Stahl's data (17), because in the present method the only force acting upon the molecule under titration is the field strength (V/cm), which "sees" only the degree of charge present in the molecule at any given pH value.

Interestingly, quite recently, similar conclusions have been reached by Jokl *et al.* (32) who have described a zone electrophoresis method, in water-alcohol solvents, by which it is possible to estimate pK's of weak or-

ganic acids and bases. Their system is rather primitive, though, since the mobility curves can be only reconstructed by a series of electrophoretic runs (at least 15) at 0.5 pH intervals in a universal buffer, using filter paper as a support. Thus, corrections for electroendosmosis and sorption by the carrier have to be introduced. Moreover, since they do not deal with amphoteric species, their theory does not provide correction of mobility data in case of adjacent pK's in the same molecule. Nevertheless, even though they have used a different mathematical approach, their conclusions on the calculations of pK values from mobility data are quite similar to the ones we have outlined.

Discussion

Several advantages are inherent to the present method:

- a) a "titration" or "pH-mobility curve" is developed within a single experiment, as opposed to 20-30 experiments in conventional electrophoresis;
- b) in order to be titrated, a protein preparation does not need to be homogeneous, as in conventional potentiometric titrations, since each component of the mixture will develop its own pH-mobility curve independently from the other species;
- c) by developing zymogram techniques, protein extracts can be analyzed at the early stages of a purification protocol, thus determining the proper pH conditions for subsequent purification work by charge-dependent methods, such as electrophoresis, isotachopheresis, equilibrium IEF and ion-exchange chromatography;
- d) when running interacting species, the stoichiometry of the complex, its half-life, pH range of stability and ionic groups involved in the binding can all be estimated quite accurately within a single experiment;
- e) when running a protein and its genetic mutant in a mixture, this is equivalent to performing a "differential titration curve". In fact, if the charge difference between the two species is already known, simple mobility measurements at any given pH will allow direct measurement of the num-

ber of protons lost or acquired by the protein at that pH (taking as reference or "zero" point the isoelectric point of the macromolecule). As an example, by running "differential titrations" of mixtures of HbA, HbS and HbC, we had previously stated that, in going from the pI plane (pH 7.0) to pH 9.0, HbA had shaken off some 12 ± 2 protons. On the basis of the known amino acid sequence of HbA, we can now make the following calculations: four H^+ will be released by 38 His residues, two H^+ by 4 $-NH_2$ termini, two H^+ by 2 β^{93} -SH groups and two H^+ by 44 Lys residues, totalling some 10 protons (notice that they all add up, since we are measuring anionic mobilities!). Given the uncertainty of early measurements, the agreement between theoretical and experimental data does not seem so bad.

The major limit of the present technique is that at the moment we have no theory for the analysis of such complex titration curves as developed by polyelectrolytes. It should be possible to work one out, perhaps on the basis of the Linderström-Lang equation, but a lot more theoretical and experimental work has to be done.

Acknowledgements

Supported in part by grants No. 78.02249.04 and 78.01533.06 from Consiglio Nazionale delle Ricerche (CNR, Roma). E. Gianazza is a fellow of the National Medical Research Council. It is our pleasure to recall here the collaboration with Drs. R. Krishnamoorthy and D. Labie, with whom part of this work was developed during a beautiful summer in Paris.

References

1. Rosengren, A., Bjellqvist, B., Gasparic, V.: in Radola, B.J., Graesslin, D. (eds.) *Electrofocusing and Isotachopheresis*, pp. 165-171, W. de Gruyter, Berlin 1977.
2. Righetti, P.G., Krishnamoorthy, R., Gianazza, E., Labie, D.: *J. Chromatogr.* **166**, 455-460 (1978).
3. Krishnamoorthy, R., Bianchi Bosisio, A., Labie, D., Righetti, P.G.: *FEBS Letters* **94**, 319-323 (1978).
4. Righetti, P.G., Gacon, G., Gianazza, E., Lostanlen, D., Kaplan, J.C.:

- Biochem. Biophys. Res. Commun. 85, 1575-1581 (1978).
5. Righetti, P.G., Menozzi, M., Gianazza, E., Valentini, L.: FEBS Letters 707, 51-55 (1979).
 6. Righetti, P.G., Gianazza, E.: in Peeters, H. (ed.) Protides of the Biological Fluids, vol. 27, Pergamon Press, Oxford, in press.
 7. Von Smoluchowski, M.: Bull. Acad. Cracovil, 182-199 (1903).
 8. Debye, P., Hückel, E.: Physik. Z. 25, 49-60 (1924).
 9. Hückel, E.: Physik. Z. 25, 204-220 (1924).
 10. Henry, D.C.: Proc. Royal Soc. A733, 106-119 (1931).
 11. Jacob, J.J.C.: Biochem. J. 47, 83-94 (1947).
 12. Jacob, J.J.C.: Biochem. J. 42, 71-79 (1942).
 13. Longworth, L.G., Cannan, R.K., MacInnes, D.A.: J. Amer. Chem. Soc. 62, 2580-2590 (1940).
 14. Brinton, Jr., C.C., Lauffer, M.A.: in Bier, M. (ed.) Electrophoresis, vol. 1, pp. 427-492, Academic Press, New York 1959.
 15. Furchgott, R.F., Ponder, E.: J. Gen. Physiol. 24, 447-457 (1941).
 16. Volkin, E.: J. Biol. Chem. 175, 675-681 (1948).
 17. Stahl, E.: Angew. Chem. Int. Ed. 3, 784-791 (1964).
 18. Stahl, E.: J. Chromatogr. 165, 59-73 (1979).
 19. Michl, H.: Monat. Chemie 83, 210-220 (1952).
 20. Kolin, A.: in Glick, D. (ed.) Methods of Biochemical Analysis, vol. 6, pp. 259-288, Wiley, Interscience, New York 1958.
 21. Friedli, W., Schumaker, E.: Hel. Chim. Acta 44, 829-856 (1961).
 22. Ogston, A.G.: Nature 157, 193-194 (1946).
 23. Singer, S.J., Campbell, D.H.: J. Amer. Chem. Soc. 74, 1794-1798 (1952); 75, 5577-5580 (1953); 77, 3499-3503 and 3504-3508 (1955); 77, 4851-4854 (1955).
 24. Singer, S.J., Eggman, L., Campbell, D.H.: J. Amer. Chem. Soc. 77, 4855-4859 (1955).
 25. Pepe, F.A., Singer, S.J.: J. Amer. Chem. Soc. 78, 4583-4587 (1956).
 26. Baker, M.C., Campbell, D.H., Epstein, S.I., Singer, S.J.: J. Amer. Chem. Soc. 78, 312-316 (1956).
 27. Hedlund, K.W., Nicholson, D.E.: J. Chromatogr. 162, 76-80 (1979).
 28. Righetti, P.G., Krishnamoorthy, Lapoumeroulie, C., Labie, D.: J. Chromatogr. 177, 219-225 (1979).
 29. Rüchel, R., Steere, L.R., Erbe, E.F.: J. Chromatogr. 166, 563-575 (1978).
 30. Baumann, G., Chrambach, A.: Anal. Biochem. 70, 32-41 (1976).
 31. Bianchi Bosisio, A., Snyder, S., Righetti, P.G.: J. Chromatogr., in press.
 32. Jokl, V., Dolejšová, J., Matusová, M.: J. Chromatogr. 172, 239-248 (1979).

PARTITIONING AND ELECTROPHORESIS IN FLEXIBLE POLYMER NETWORKS

H.J. Bode

Zoologisches Institut der Universität, Im Neuenheimer Feld 230
D-6900 Heidelberg 1 , Germany

Introduction

In a recent publication, molecular sieving in polyacrylamide gel electrophoresis was inferred from the properties of a hypothetical 'viscosity-emulsion' composed of two interlacing fluid compartments endowed with different frictional coefficients (1). Following classical theories of gel chromatographic partitioning (2, 3), a static representation of internal gel geometry as given in Ogston's theory (4) was adopted. However, physicochemical data suggest high flexibility of polyacrylamide chain segments, even if crosslinked (5), and despite of an enormous viscosity of the gel as a whole (6). Hence, polyacrylamide gels behave like congested polymer solutions (7-9). In the 'viscosity-model', this was heuristically accounted for by attributing fluidity to the gel compartment in which contact between macro-ions and gel elements would take place according to Ogston's model. A more precise description which comprises the arguments needed for deduction of partitioning effects in granulated polyacrylamide gels (3, 10, 11) has to make use of physicochemically defined parameters of rubber-like gels, i.e. conformational probability, entropy, and elasticity of fluctuating chains (12). The suggested approach is based on a multiple sheet matrix of viscoelastic obstructions (of unspecified chemical composition). The influences of viscoelastic specifications of the matrix on several variables are demonstrated in diagrams, and formulae are presented to correlate mobility, partition coefficient, and 'fractional specific resistance' (= FSR) with the probability distribution of polymer conformations within single sheets. Finally, the multiple sheet model is

converted into a viscoelastic continuum in order to approximate the presumed properties of continuous polyacrylamide gels.

The Multiple Sheet Model

The multiple sheet model serves to illustrate the single parameters necessary for an understanding of viscoelastic continua. The viscoelastic matrix has to be imagined as a layer of parallel sheets each of which is composed of fluctuating polymer chains which are inserted into an unspecified backbone. Fluctuations due to thermal agitation are centred symmetrically around the median plane of each sheet. These motions of polymers give rise to elastic forces (figs.1-3) directed towards any compact object which tends to invade the volume otherwise available to the polymers for molecular reorientation. Nevertheless, macromolecules are assumed to be able to permeate through sheets in all directions. Since elastic and frictional parameters are assumed to be constant in planes oriented in parallel to the sheet layer, but to vary in direction of the electrical field vector which is perpendicular to these planes, only one unique motion axis has to be considered (s-axis). This facilitates a mathematical treatment. Only time-average parameters disregarding the influence of thermal agitation are used in the following deduction of partitioning effects based on the molecular competition for disposable volumes. The fact that elastic repulsion as well as hydrodynamic friction are functions of the degree of geometrical interference gives rise to size-sensitivity in fractionation methods which rely on these parameters.

Partition Equilibrium

As a consequence of negative concentration gradients, macromolecules can be expected to diffuse from an outer reservoir solution into the interior parts of a multiple sheet matrix until partition equilibrium is reached. In equilibrium, there is complete balance of inward and

outward transport rates and equivalence of the pertinent time-average forces. The 'invading force' due to the gradient can be inferred from Fick's law as follows:

$$R = -D \cdot \frac{dc(s)}{ds} = -\frac{k_B \cdot T}{f(s)} \cdot \frac{dc(s)}{ds} = c(s) \cdot v(s) \quad (1)$$

(R=transport rate per unit cross-section, D=diffusion coefficient, c(s)=local concentration of macromolecules, k_B =Boltzmann's constant, T=absolute temperature, f(s)=frictional coefficient, v(s)=drift velocity of macromolecules)

Since in free diffusion the gradient force would be equal to frictional force (= v·f), it follows:

$$\text{'invading force'} = -k_B \cdot T \cdot \frac{dc}{c(s) \cdot ds} \quad (2)$$

In partition equilibrium, this force is cancelled by a repulsive force which tends to sweep macromolecules out of the volume pervaded by polymer chains. The latter force can be inferred from the change in conformational probability induced by the invading macromolecule (figs.1 and 2) by means of Boltzmann's equation:

$$\Delta S = k_B \cdot \Delta \ln w(s) = k_B \cdot \Delta \ln W_2(s) \quad (3)$$

(S=entropy, w(s) and $W_2(s)$ are as defined in fig.2)

Multiplication by T yields the energy change which accompanies the process of invasion. Elastic force is obtained as the first derivative of energy along the s-axis:

$$\text{'elastic force'} = T \cdot \frac{dS(s)}{ds} = k_B \cdot T \cdot \frac{d(\ln w(s))}{ds} \quad (4)$$

The partition equilibrium is characterized by equivalence of the forces involved. Hence:

$$k_B \cdot T \cdot \frac{d(\ln w(s))}{ds} - k_B \cdot T \cdot \frac{dc}{c(s) \cdot ds} = \text{zero} \quad (5)$$

Equilibrium concentrations can be calculated from this equation when an empirical or hypothetical elastic force profile is provided, since:

$$c(s) = c_0 + \int_{-\infty}^s \left(\frac{dc}{ds} \right) \cdot ds = c_0 + \int_{-\infty}^s c(s) \cdot \frac{d(\ln w(s))}{ds} \cdot ds = c_0 \cdot w(s) \quad (6)$$

(c_0 =concentration of macromolecules in the outer reservoir)

The average concentration within the multiple sheet matrix is obtained by integration and characterizes (if relative values are compared) the 'accessibility', resp. the 'fractional available volume'

of the system:

$$K_{av} = \frac{\int_{s_1}^{s_2} c(s) \cdot ds}{c_0 \cdot \int_{s_1}^{s_2} ds} \quad (7)$$

(K_{av} =partition coefficient, resp. fractional available volume determined by gel filtration; s_1, s_2 =margins of the multiple sheet matrix)

Electrophoresis

General remarks

In electrophoresis, the partition equilibrium is disturbed by the advent of two kinds of forces: the electrokinetic force K , and the frictional force ($= v \cdot f$) which impedes the drift of macro-ions. This drift is governed by the following force equilibrium (neglecting accelerating forces and thermal agitation):

$$K + k_B \cdot T \cdot \frac{d(\ln w(s))}{ds} - k_B \cdot T \cdot \frac{dc}{c(s) \cdot ds} - v(s) \cdot f(s) = \text{zero} \quad (8)$$

In this equation, the sum of the first three items designates the 'actual driving force' ($= A(s)$) which promotes the net drift of macro-ions. Observations are restricted, in the following text, to the electrophoretic steady state which is characterized by a constant net transport rate through all cross-sections of the system:

$$R' = \text{const.} = v(s) \cdot c(s) \quad (9)$$

and by the additional condition that no elastic energy is accumulated in the course of time and no net accumulation of macro-ions takes place. Hence, the energy dissipated during migration originates entirely from the drop in electrical potential of macro-ions. The aforementioned conditions can be formalized as follows:

$$A(s) = \frac{f(s)}{c(s)} \cdot R' \quad (10)$$

$$\text{and: } \int_{s_1}^{s_2} A(s) \cdot ds = K \cdot \int_{s_1}^{s_2} ds \quad (11)$$

Insertion of eq.(10) into eq.(11) leads to:

$$R' = \frac{K \cdot \int_{s_1}^{s_2} ds}{\int_{s_1}^{s_2} \frac{f(s)}{c(s)} \cdot ds} \quad (12)$$

Calculation of R' requires the knowledge of local frictional coefficients of the sheet matrix. Although the actual relationship is not known, it can tentatively be assumed that $f(s)$ depends linearly on the fraction of polymer conformations which are prevented by the presence of a macro-ion, i.e. on $(1 - w(s))$. Therefore, we can define:

$$f(s) = f_0 + f_0 \cdot k \cdot (1 - w(s)) \quad (13)$$

(f_0 = frictional coefficient in free solution; k = proportionality constant)

Since electrophoretic steady-state concentrations deviate from the equilibrium concentrations, the value of R' has to be calculated by an iterative approximation procedure. This can start from the ratios of $(f(s)/c(s))$ obtained in equilibrium. Integration (resp. summation) of these values according to eq.(12) leads to a first estimate of R' . Values of $A(s)$ can then be calculated according to eq.(10); subtraction of K and of elastic force from these values yields approximative steady state gradient forces which can be converted into a preliminary concentration profile along the s -axis. Using this profile, a second round of approximation can be started. After calculation of the velocity profiles within viscoelastic sheets, the empirically measurable relative mobility of macro-ions can be obtained as follows:

$$u_{rel} = \frac{\int_{s_1}^{s_2} ds}{v_0 \cdot \int_{s_1}^{s_2} \frac{1}{v(s)} \cdot ds} = \frac{f_0 \cdot \int_{s_1}^{s_2} ds \cdot \int_{s_1}^{s_2} ds}{\int_{s_1}^{s_2} \frac{f(s)}{c(s)} \cdot ds \cdot \int_{s_1}^{s_2} c(s) \cdot ds} \quad (14)$$

Compound sheets

The combination of several viscoelastic sheets into 'compound sheets' (fig.8) exemplifies the effect of overlap of neighbouring, independently fluctuating units. Overlap tends to smooth profiles of force and velocity; this levelling effect is due to the partial cancellation of positive and negative elastic forces in the space between neighbouring sheets provided additivity of forces can be assumed. The latter condition requires a 'phantom'-like behaviour of polymer chains (comp.ref.12), i.e. the capability to interdigitate and to penetrate one another without having mutual influence on their respective conformations. Under these conditions, a 'compound probability' $\bar{w}(s)$ can be defined for the overlap region:

$$\bar{w}(s) = w_1(s) \cdot w_2(s) \cdot w_3(s) \cdot \dots \quad (15)$$

The 'compound frictional coefficient' within overlap regions may be calculated by insertion of $(1 - \bar{w}(s))$ into eq.(13); however, an alternative convention would be suitable as well.

Viscoelastic continuum

As illustrated by the 'compound sheets', inhomogeneities of parameters correlated with $w(s)$ are levelled off by overlap of independent sheets. In contrast to the afore-mentioned specifications concerning 'compound sheets', a 'viscoelastic continuum' can be imagined as an extended unit of overlapping sheets in which the local variations of $\bar{w}(s)$ and of dependent parameters are completely cancelled out due to mutual congestion. Only on the margins will elastic force follow the one-sided half-profile of a single, independent sheet; in the interior, the elastic force will be zero.

Fractional specific resistance

The 'fractional specific resistance' (=FSR) which was introduced, recently, to characterize resistance against deformation and

dislocation of polymers on the basis of a 'viscosity-emulsion' (1) can also be calculated for the multiple sheet matrix by inserting the terms deduced for u_{rel} and for K_{av} into the defining equation:

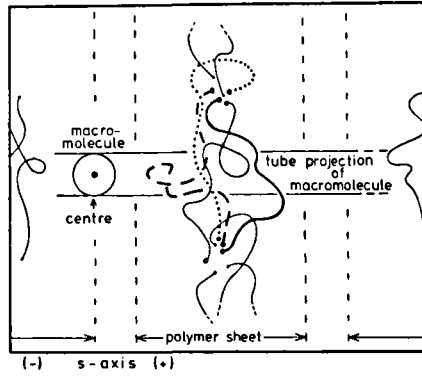
$$FSR = \frac{1 - u_{rel}}{1 - K_{av}} \cdot \frac{1}{u_{rel}} = \frac{\int \frac{f(s)}{c(s)} \cdot ds \cdot \int c(s) \cdot ds - f_0 \cdot \int ds \cdot \int ds}{f_0 \cdot \int ds \cdot \int (1 - \bar{w}(s)) \cdot ds} \quad (16)$$

Results and Discussion

As outlined graphically in figs.1-4, and theoretically in eqs.1-5, it is possible to deduce the partitioning effect exerted within loose polymer networks on diffusing macromolecules from elastic molecular forces of the polymers. These forces are due to the spatial restriction of the thermally induced conformational fluctuations of polymer chains. The inherent loss of conformational probability can be linked with entropy and elastic energy through Boltzmann's equation. This conforms with theories concerning strain elasticity of rubbers (12). The dynamic exclusion of macromolecules, suggested here, contrasts with the strictly geometric mechanism assumed in earlier theories of gel chromatographic partitioning (2-4). In the light of the high flexibility found in polyacrylamide chains (5, 9), it seems that Ogston's theory can only be applied to these polymers if it is regarded as an approximate 'frozen-in' representation of the gel interior.

Fluctuations of polymers have bearing on the presumed mechanisms of electrophoretic migration of macro-ions within gels. In earlier theories, retardation of macro-ions was attributed to the effectiveness of 'barriers' forcing the macro-ions to follow tortuous paths (10, 13, 14). In contrast, macro-ions are now assumed to migrate along straight field-lines. Minor deviations from this direction due to thermal agitation need not be considered in the sheet layer model because of its particular construction: the relevant parameters do not vary in directions perpendicular to the field vector. There are major differences between the sheet layer model and the 'viscosity-

Fig. 1



(see the legends on the opposite page)

Fig. 2

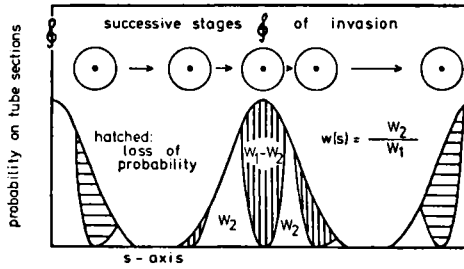


Fig. 3

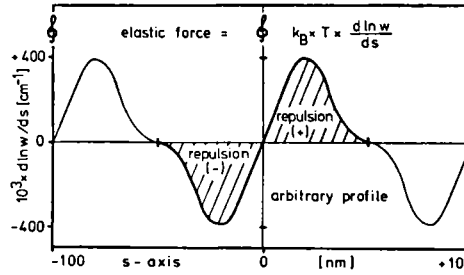


Fig. 4

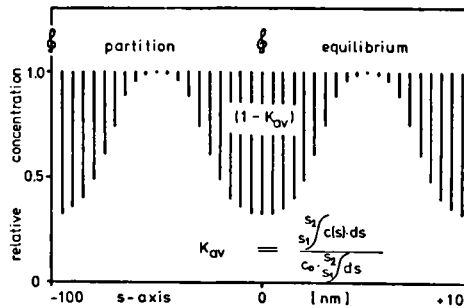


Fig.1 : Conformational changes of a polymer chain which fluctuates symmetrically around the median plane of a viscoelastic sheet. Neighbouring sheets are indicated at the right and left margins. Invading macromolecules interfere with the spontaneous motions of the chains.

Fig.2 : Probability density of polymer conformations along the s-axis. The integral of the (arbitrary) bell-shaped curve denotes the probability that during migration through the sheet the macromolecule interferes with polymers. Depending on the size of the macromolecule and on the position of its centre relative to the sheet centre, a certain number of conformations will be prevented (hatched areas). The residual freedom for spontaneous motions is characterized by the ratio: $w(s) = W_2(s)/W_1$. Positions of the median planes of viscoelastic sheets with regard to (s) are indicated by violin clefs.

Fig.3 : Elastic force opposed to invading macromolecules. Elastic force can be calculated from diagrams as shown in fig.2 by means of eq.(4). The numerical scales on the ordinate and abscissa as well as the shape of the curve are arbitrary, but they are used as the basis for all subsequent calculations.

Fig.4 : Partitioning of macromolecules between separate sheets. The equilibrium distribution of macromolecules was calculated from the elastic force profile shown in fig.3 according to eq.5. Relative concentrations are indicated by the end positions of vertical bars. The blank area stands for the 'accessibility' of the system, hence for K_{av} .

model' suggested before (1). The interfaces separating the contact-zones (which surround polymers according to Ogston's theory) from non-contact zones are now assumed to fluctuate in concert with the polymer chains instead of remaining stationary. In particular, this means that fluctuations occur at higher rates than the net drift velocity of macro-ions. Interaction of macromolecules with polymers can therefore be visualized as a sort of 'thermal palpitation' of macro-ions rather than shoving aside of stationary polymers. Although some other properties of the sheet layer model may seem hypothetical, they are nevertheless pedagogically useful. Due to the steady state condition, stable concentration gradients are produced in the spaces between the sheets which heavily influence the 'actual driving force' $A(s)$ which had been assumed to be constant in the former model. As evidenced by the figures (figs.5-9), $A(s)$ can even be stronger than the electrokinetic force K . This can give rise to migration velocities which are higher in the centres of obstructions

Figs.5-9 : Steady state profiles of $c(s)$ (=concentration of macro-ions, vertical bars), of $A(s)$ (=actual driving force, broken line), and of $v(s)$ (=migration velocity, dashed line) within single units of an infinite viscoelastic sheet matrix. All plotted values have been calculated in two non-computerized rounds of approximation and have been normalized as values relative to free solution. Unless otherwise stated, the calculations were based on the following numerical assumptions: (a) the elastic force effective in each single sheet is represented by the curve in fig.3 ; (b) the frictional coefficient obeys eq.(13) with inserted values of k as stated in the figures; (c) the electrokinetic force K is equal to $10^5 \cdot k_B \cdot T$ (dyn) corresponding to a total number of 254 elementary charges per macro-ion at a field strength of 10 volt/cm (this high value was chosen in order to produce susceptible concentration gradients in the figures).

Fig.5 a-c : Effect of hydrodynamic friction.

The average migration velocity is lowered by enhancement of k (fig.5 a+b). Absence of partitioning forces (resp.elasticity) is able to smooth the profiles of concentration and velocity (fig.5c).

Fig.6 a-c : Effect of elasticity.

Reduction of the elastic force to 1/10 of the values shown in fig.3 levels velocity up (figs.6a+b). Enhancement of k is able to restore low velocity, but leads to a different velocity profile.

Fig.7 a-c : Effects of charge and size.

Reduction of size of the macro-ion weakens the geometrical interference with polymers and shifts velocity up. Reduction of electric charge (or voltage gradient) minimizes the deviations of the steady state concentrations from partition equilibrium.

Fig.8 a-c : Effects of sheet density and overlap of sheets.

When single viscoelastic sheets are replaced by 'compound sheets', the average velocity drops. Within the 'compound sheets', the profiles of $v(s)$, $A(s)$, and $c(s)$ are smoothed due to the mutual cancellation of elastic forces in regions of overlap (fig.8c).

Fig.9 : Viscoelastic continuum.

The 'viscoelastic continuum' is an extended 'compound sheet' with modified specifications since $\bar{w}(s)$, $f(s)$, and the elastic energy of invaded macromolecules are assumed to be completely constant within the interior parts of the continuum. The tendency to level off variations of $A(s)$, $c(s)$, and $v(s)$ is much more pronounced than in the quintuple sheet of fig.8c. Real polyacrylamide gels may represent viscoelastic continua of much larger dimensions than the single unit shown in the figure.

than in the free solution between separate sheets. The explanation for this apparent paradox is that macro-ions are piled up before the obstacles thus storing the energy which helps them to overcome the peak values of elastic or frictional resistance within the sheets. The influences of hydrodynamic friction, elastic repulsion, of

Fig. 5
(see the legends on the opposite page)

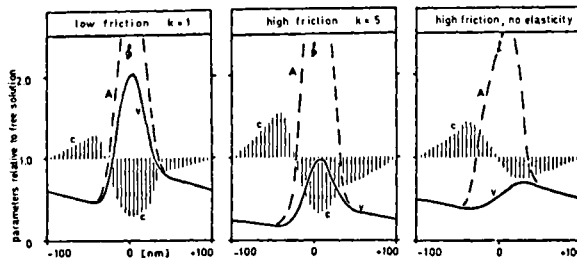


Fig. 6

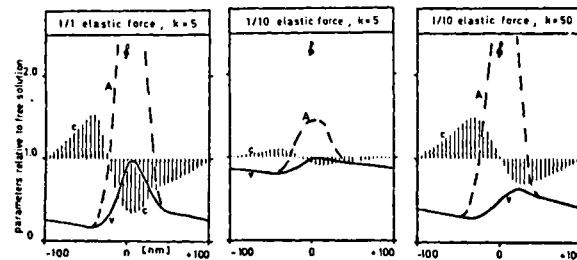


Fig. 7

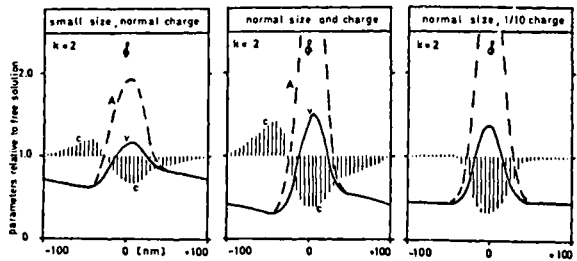


Fig. 8

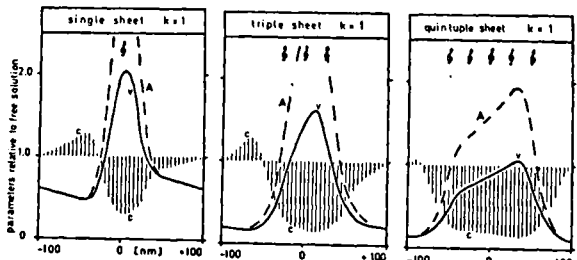
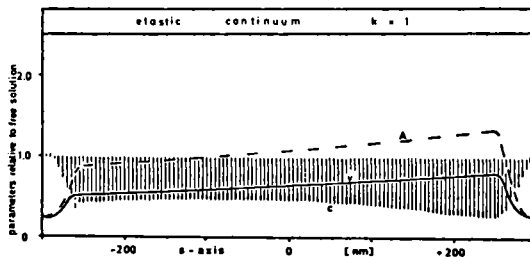


Fig. 9



charge and size of the macro-ions, and of density and arrangement of polymer sheets on the obtained velocity profiles are rather complex as shown by the figures (fig.5-8). Parameters which would characterize the matrices on the macroscopic level, i.e. the level which is amenable to experimental analysis, are summarized in table 1. It can be seen that both hydrodynamic friction (fig.5) and elastic repulsion (fig.6) are able to lower the overall mobility within the sheet matrix and to contribute to the level of FSR which is always larger than the proportionality constant k defined in eq.(13). Certain correlations exist between specifications of the sheet matrix and the velocity profiles obtained by calculation. Extreme peak velocities within the sheets are observed in combination with strong elastic repulsion which is the cause for lowered concentrations. This affects FSR, as well, which is sensitive to inhomogeneous distribution of macro-ions within the system. Under conditions of strong hydrodynamic friction and weak elastic repulsion, the obtained profiles of velocity and concentration are rather smooth; this favours proximity of the values of FSR and k . The influence of elastic repulsion on the values of FSR and u_{rel} is mediated by the variability of concentration due to partitioning between separate sheets.

Table 1

Macroscopic parameters of multiple sheet matrices calculated from the values shown in figs.5-9

	a	b	c	a	b	c	
Fig.5 u_{rel}	0.71	0.29	0.50	0.29	0.97	0.41	u_{rel} Fig.6
k_{av}	0.82	0.82	un-	1.82	0.97	0.97	k_{av}
FSR	2.2	13.2	defi-	13.2	5.1	60.7	FSR
k	1.0	5.0	ned	5.0	5.0	50.0	k
Fig.7 u_{rel}	0.81	0.50	0.57	0.71	0.32	0.32	u_{rel} Fig.8
k_{av}	0.91	0.82	0.82	0.82	0.60	0.39	k_{av}
FSR	2.6	5.6	4.1	2.2	5.1	3.4	FSR
k	2.0	2.0	2.0	1.0	1.0	1.0	k
Fig.9 u_{rel}	0.56	k_{av}	0.38	FSR	1.2	k	1.0

Both parameters depend on the product of two integrals in one of which $c(s)$ is the denominator, whereas in the other one it is the numerator. By consequence, the product will always be larger in cases of pronounced variation of the polymer distribution along the s -axis which is the origin of inhomogeneous distribution of macromolecules. Since uneven distribution is caused by the limited amplitude of polymer fluctuations around sheet centres the spacings of which do not vary, the strongly compartmented multiple sheet model is not likely to apply to polyacrylamide gels; this would require the existence of a stiff backbone in the gel which holds the sheets apart from one another. Polyacrylamide gels are presumably closer to an extended viscoelastic continuum. This point is of particular interest with respect to the validation of FSR. As demonstrated in fig.9, the 'actual driving force' $A(s)$ is very close to the electrokinetic force K , and $v(s)$ and $c(s)$ are almost constant in the interior of the continuum. Evidently, they would assume the values of u_{rel} , resp. of K_{av} in the limiting case of an infinite thickness of the continuum. Under these conditions, FSR no longer depends on $w(s)$, $f(s)$, or $c(s)$ since these constants can be reduced in the term which defines FSR :

$$\begin{aligned}
 \text{FSR} &= \frac{\frac{f_0}{c_0} \cdot \int \frac{1+k-k\bar{w}}{\bar{w}} \cdot ds \cdot c_0 \cdot \int \bar{w} \cdot ds - f_0 \cdot \int ds \cdot \int ds}{f_0 \cdot \int ds \cdot \int (1-\bar{w}) \cdot ds} = \\
 &= \frac{(1-\bar{w}) \cdot k \cdot \int ds \cdot \int ds}{(1-\bar{w}) \cdot \int ds \cdot \int ds} = k \quad (17)
 \end{aligned}$$

This identity documents an intimate relationship in the definitions of FSR and k :

$$k = \frac{f_p - f_0}{f_0} \cdot \frac{1}{1 - \bar{w}} \quad (18) \quad \text{and} \quad \text{FSR} = \frac{f_p - f_0}{f_0} \cdot \frac{1}{1 - K_{av}} \quad (19)$$

In either case, the apparent frictional coefficient of the overall system ($=f_p$) which disregards temporal variations or spatial compartmentation of $f(s)$ is converted into a parameter which characterizes the state of actual interference or contact between macro-ions and polymers. In the former case, k is obtained by dividing the term

$(f_p - f_0)/f_0$ (which is analogous to 'specific viscosity', see ref.1) by the time-average probability of geometric interference, i.e. by $(1 - \bar{w})$; in the latter case, FSR is obtained from the same term by dividing by the expected space-average probability of geometric interference, i.e. by $(1 - k_{av})$. This analogy of definitions reveals that illustration of the gel interior as a 'viscosity-emulsion' traces a momentary 'frozen-in' picture of the dynamic interaction process which combines, in reality, the effects of elastic repulsion (due to spontaneous reorientations of polymer chains) with the hydrodynamic frictional effects (due to forced reorientations under the electrokinetic pressure). According to this distinction, gel filtration and gel electrophoresis can be assumed to make use of different molecular properties in order to achieve fractionation of macromolecules. By the establishment of an identity of FSR and k (within the limitations imposed by definition of a viscoelastic continuum), FSR is shown to be a legitimate and physically meaningful measure of hydrodynamic friction in gels.

References

1. Bode, H.J.: Z.Naturforsch. 34c, 512-528 (1979).
2. Laurent, T.C., Killander, J.: J.Chromatogr. 14, 317-330 (1964).
3. Fawcett, J.S., Morris, C.J.O.R.: Sep.Sci. 1, 9-26 (1966).
4. Ogston, A.G.: Trans.Faraday Soc.(Aberdeen) 54, 1754-1757 (1958).
5. Hecht, A.M., Geissler, E.: J.Physique 39, 631-638 (1978).
6. Bacri, J.C., Dumas, J., Levelut, A.: J.Physique (Lettres) 40, 231-235 (1979).
7. Munch, J.P., Candau, S., Herz, J., Hild, G.: J.Physique 38, 971-976 (1977).
8. Daoud, M., Cotton, J.P., Farnoux, B., Jannink, G., Sarma, G., Benoit, H., Duplessix, R., Picot, C., de Gennes, P.G.: Macromolecules 8, 804-818 (1975).
9. Kulicke, W.M.: Makromol.Chem. 180, 543-549 (1979).
10. Morris, C.J.O.R.: Prot.Biol.Fluids 14, 543-551 (1966).
11. Morris, C.J.O.R., Morris, P.: Biochem.J. 124, 517-528 (1971).
12. Flory, P.J.: Proc.R.Soc.Lond. A351, 351-380 (1976).
13. Giddings, J.C., Boyack, J.R.: J.Theoret.Biol. 2, 1-6 (1962).
14. Rodbard, D., Chrambach, A.: Proc.Nat.Acad.Sci.U.S. 65, 970-977 (1970)

DOUBLE ONE-DIMENSIONAL SLAB-GEL ELECTROPHORESIS

K. Altland and R. Hackler

Institute of Human Genetics, University of Giessen,
Schlangenzahl 14, D-6300 Giessen, Fed. Rep. Germany

Introduction

The high resolution obtained by PAGE and PAG electrofocusing of complex mixtures of proteins as the physiological body fluids is well known. In the usual case, however, e.g. serum, saliva, urine, amniotic fluid, etc., the total number of primary gene products and their position variants due to genetic, ligand, conformational and/or other variation is so high that considerable overlap of individual proteins makes their individual identification difficult if not impossible. This problem is overcome to a considerable degree by means of specific staining techniques, immunofixation or by increasing the resolution by combination of two electrophoretic techniques to obtain two-dimensional patterns. There still remain, however, problems and drawbacks which need to be eliminated: For instance, specific staining techniques are not available for every individual protein, immunofixation is limited by the availability of good specific antisera and two-dimensional techniques are very time consuming thus permitting the analysis of only a very few samples within a usual working day.

With the development from tube-gel electrophoresis and electrofocusing to slab-gel electrophoresis and electrofocusing another interesting combination of electrophoretic techniques has become possible which is suggested to be called double one-dimensional slab-gel electrophoresis.

Multiple step one-dimensional separation is an old standard procedure to purify a compound from a complex mixture of "impurities". Double one-dimensional electrophoresis could be a set of two consecutive electrophoretic steps within such a process to isolate a compound. It has been success-

fully used many times in many laboratories as far as the handling of individual samples is concerned. Double one-dimensional slab-gel electrophoresis provides a new perspective in gel electrophoresis different from single step procedures, two-dimensional electrophoresis as well as from double one-dimensional electrophoresis of individual samples as used by the rod-gel techniques.

The term double one-dimensional slab-gel electrophoresis shall designate the consecutive combination of two electrophoretic slab-gel techniques in one dimension. The analytical principle is that one fraction of the electropherogram of a set of many samples obtained by the first electrophoretic step is used as sample for the second slab-gel electrophoretic step. The principle difference to two-dimensional electrophoresis is that by the latter the whole electropherogram of one individual sample obtained by the first electrophoretic technique is used as sample for the second electrophoretic technique in the second dimension. Looking at a two-dimensional electropherogram one compares position and intensity of many different compounds from one individual sample. Looking at a double one-dimensional slab-gel electropherogram one compares position and intensity of one individual compound, e.g. product of one gene locus, from many different samples or individuals.

As there are a lot of slab-gel electrophoretic techniques available the number of theoretical combination for double one-dimensional electrophoresis is rather large although not useful in every case. The consecutive combination of PAG electrofocusing and PAGE has been used by Altland et al. (1) to demonstrate and compare basic low molecular weight compounds from sera focusing in the range of IgG where they remain usually hidden by high molecular weight immunoglobulins. The reverse consecutive combination PAGE and PAG electrofocusing appears to be of special interest for the geneticist because it provides at the level of up to date highest resolution information on interindividual variation of primary gene products within a genetically heterogeneous species.

Principle of the Method. Example: Human Transferrin (Tf)

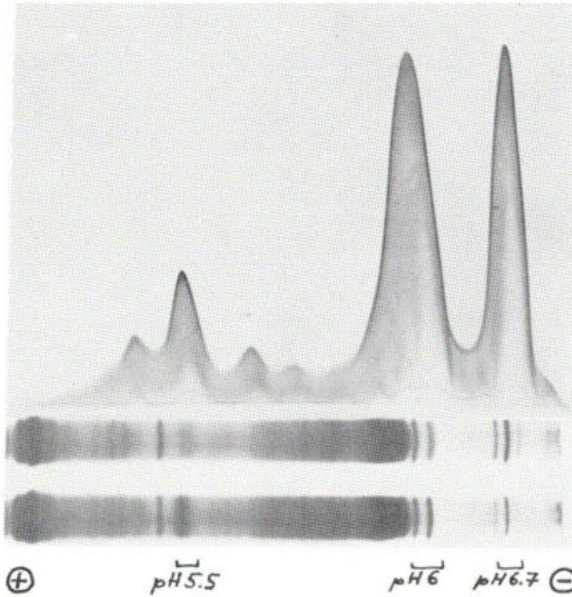


Fig.1: Crossed immunoelectrophoresis of human serum transferrin after PAG-electrofocusing of 2 μ l serum in 4.5 M urea. Two control patterns of the first dimension stained for protein are shown at the bottom.

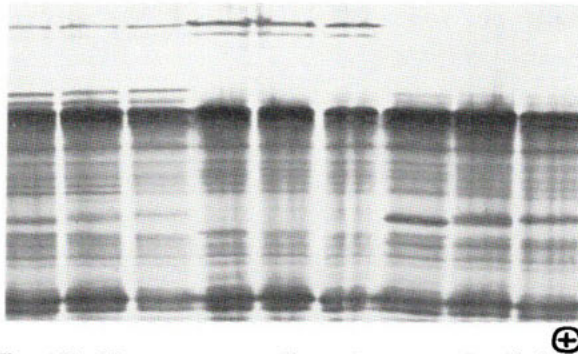


Fig.2: PAG-EF in 4.5 M urea of 3 sera of different Tf-phenotype. Samples were applied at the cathodic end of the gel. 1-3: untreated sera; 4-6: same sera incubated in 60 mM $\text{Na}_2\text{-EDTA}$; 7-9: same sera treated in 1 mM FeCl_3 . Note the change of the patterns in the range assumed to be $\text{Fe}_0\text{-Tf}$, $\text{Fe}_1\text{-Tf}$ and $\text{Fe}_2\text{-Tf}$.

$\text{Fe}_2\text{-Tf}$. There are two $\text{Fe}_1\text{-Tf}$ compounds diminished in the EDTA- and $\text{FeCl}_3\text{-}$ treated sera. The 3 Tf-phenotypes are best distinguished at the level of $\text{Fe}_2\text{-Tf}$, less at the level of $\text{Fe}_1\text{-Tf}$ and not at all at the level of $\text{Fe}_0\text{-Tf}$.

Human Tf is an extensively studied glycoprotein of the serum with two binding sites for iron. Usually only one third to one fourth of these binding sites are saturated. As a consequence at least four different molecular forms of Tf are expected to exist in sera with free iron binding capacity, e. g. the apotransferrin or $\text{Fe}_0\text{-Tf}$, two forms of $\text{Fe}_1\text{-Tf}$ and the completely saturated $\text{Fe}_2\text{-Tf}$. These different molecular forms cannot be separated by conventional PAGE. A good separation, however, can be obtained using PAG-electrofocusing as demonstrated in figures 1 and 2. The shape of the

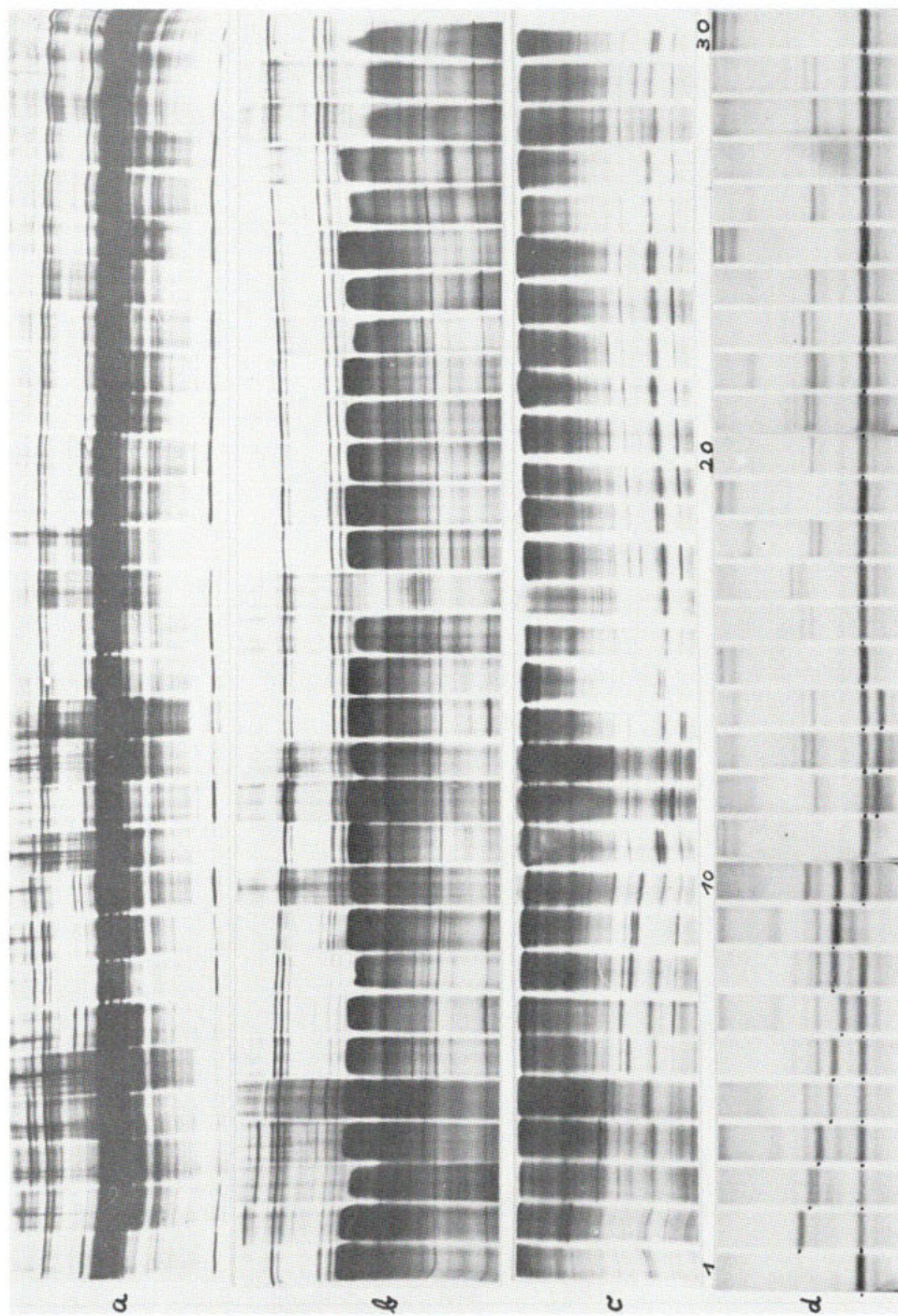
Fig.3: a) PAG-EF in 8 M urea of sera of different Tf-phenotype. b) PAG-EF in 4.5 M urea of the same sera shown in fig. 3a). c) PAG-EF in 4.5 M urea of the same sera shown in fig. 3a) after treatment with FeCl_3 . d) PAG-electrophoresis of the same sera shown in fig. 3a). Tf-zones are indicated by dots.

In the 8 M urea gel there are only Fe_0 -Tf- and one of the two Fe_1 -Tf-compounds. The other Fe_1 -Tf-compound and the Fe_2 -Tf-compounds are not detected. In the 4.5 M urea gel with untreated sera an additional Fe_1 -Tf-compound appears and - at a low level - the Fe_2 -Tf-compounds which in many samples are almost completely covered by the background produced by other proteins. In the 4.5 M urea gel with FeCl_3 -treated sera the contrast between Fe_2 -Tf-compounds and background is increased but identification remains difficult due to confusion by variation of non-Tf-compounds. Note that many of the Tf-variants seen in 3c) cannot be detected in the 8 M urea gel (3a)).

crossed immunoelectrophoresis pattern of figure 1 and the separation of the Fe_0 -Tf into several (up to 5) zones in the electrofocusing pattern indicate that additional molecular forms of Tf exist which may reflect variation within the non-aminoacid building blocks of the molecule. From figure 1 and 2 one can conclude that only Fe_0 -Tf and part of the Fe_1 -Tf compounds as well as the major fraction of Fe_2 -Tf can be demonstrated by one-dimensional PAG electrofocusing. The rest is hidden by the background mainly produced by albumin.

From figure 2 it can be also concluded that two molecular forms of Fe_2 -Tf exist in different individuals or in in the same serum sample which poorly separate at the level of Fe_1 -Tf and not at all at the level of Fe_0 -Tf. Family data have evidently shown that they are genetically determined.

Figure 3 demonstrates the separation of a series of 18 different Tf-variants in various phenotypic combinations by four different methods (2, 3). Comparing figure 3b and c with 3d the striking difference in sensitivity for the demonstration of Tf-variants in favor of PAG electrofocusing is evident. This is especially the case for those variants which are not at all detected by PAGE (see figure 4). Looking at the patterns of figure 3b and c it is obvious that the focusing region of Fe_0 -Tf and Fe_1 -Tf are much less sensitive for detecting the variants separated at the level of Fe_2 -Tf. Comparing figure 3a with 3b there is no evident difference in the sensitivity for detecting variants as far as only the focusing region of Fe_0 -Tf and Fe_1 -Tf is concerned. As there is no detectable Fe_2 -Tf in the 8 M urea gels



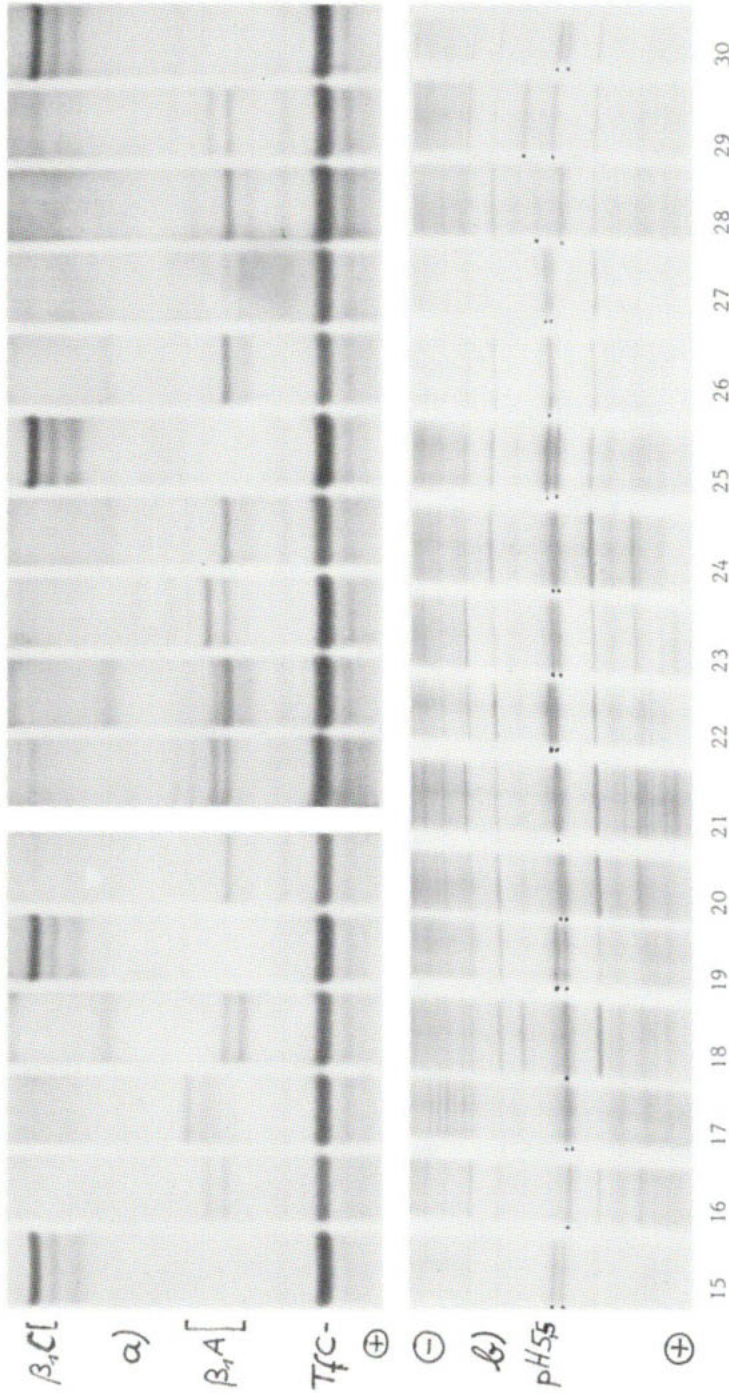


Fig.4: Detail from fig.3. a) Samples No. 15-30 from fig. 3d). b) Identical samples from fig. 3c). Note that there is no variation of Tf in the PAG-electrophoresis pattern (a) while 12 different Tf-phenotypes are obtained by PAG-EF of Fe_2 -Tf in 4.5 M urea. Tf-compounds in 4b) are indicated by dots. Samples No.15,19,25 and 30 are identical as well as samples No. 20 and 24.

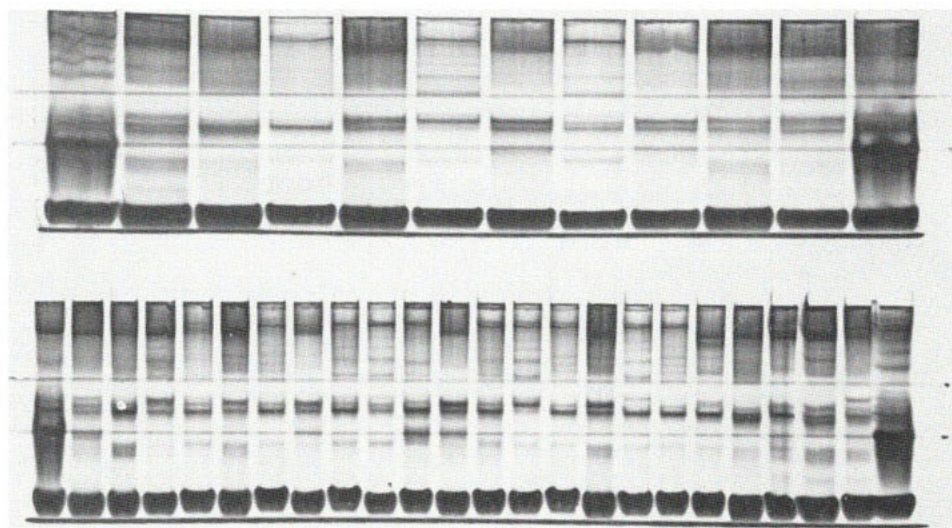


Fig.5: Short distance PAG-electrophoresis as first separating step to obtain routine double-one-dimensional patterns of transferrin. Albumin has migrated 3 cm. The gel strip with the Tf-region to be transferred to the EF-gel is indicated. Note that the extreme right and left samples contain hemoglobin at a level visible in unstained gels. The Hb-marker is used as a guide for reproducible positioning of the gel strips. The upper gel contains 12, the lower gel 24 samples which had been applied using a 12-unit multiple syringe. 4 of these gels are run simultaneously in the PAG-electrophoresis system HAVANA (DESAGA, Heidelberg). Two properly adjusted variable multiple syringes for multiple handling of samples are accessory of this high speed vertical PAGE-system.

it follows that the latter gels are less sensitive than 4.5 M urea gels for detecting the variants used in this comparative study.

From figure 3b, c and d it can be followed that the detection of electrophoretic variants by one-dimensional PAG electrofocusing is very difficult and impossible in some cases when a variant Tf-compound occupies a position identical with that of a non-Tf-compound.

This problem is overcome by double one-dimensional electrophoresis. Figure 5 demonstrates a short distance PAGE and figure 6 a long distance PAGE of sera from different individuals. The strip indicated in figure 5 which contains the Tf region and a reduced number of non-Tf-compounds is eliminated

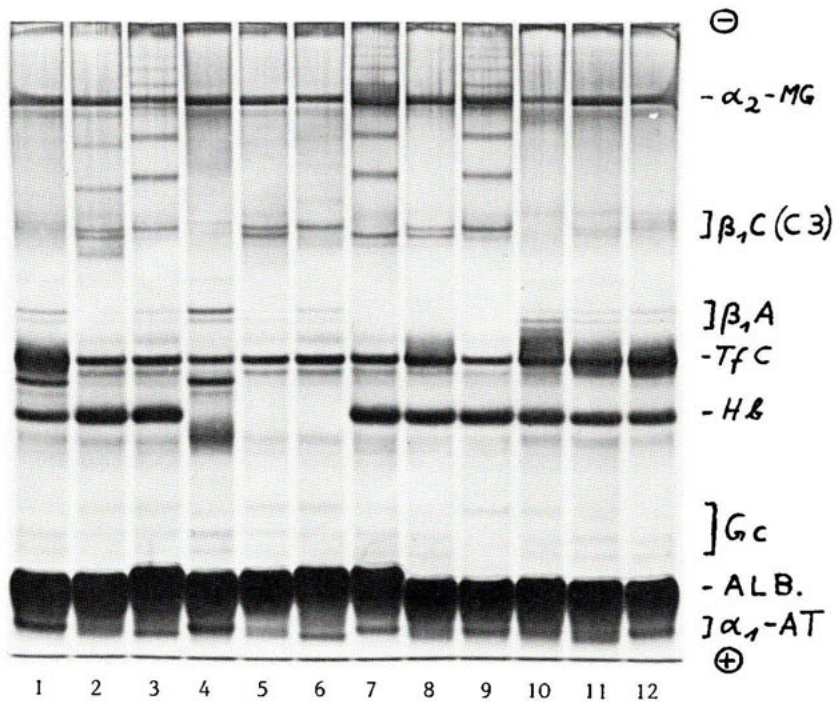


Fig.6: PAG-electrophoresis ($T=5$, $C=3$) of 1 μ l serum samples with a migration distance of 10 cm for albumin. Samples No. 1-3 are identical with No. 4-6 except that hemoglobin has been added to 1-3 as well as to samples No. 7-12 to demonstrate genetically determined haptoglobine- phenotypes as Hb-Hp-complexes (No.1:Hp1-1;No.2:Hp2-1;No.3:Hp2-2). Note that this separation distance is sufficiently large to cut out proper strips also for other non-Tf- proteins and thus to obtain high resolution EF-patterns by the double-one-dimensional slab gel technique.

from the unstained gel and used as sample for slab-gel PAG electrofocusing. The result is seen in figure 7 - 9. In figure 7 the method is used as a screening technique. Short distance PAGE is performed during the pre-focusing of the electrofocusing gel. Using this screening method more than 2.500 sera from different populations were screened for Tf-variants by three workers of our laboratory within one week including all working steps from thawing of the sera till documentation on film, data sheets, conservation of the gels by drying and repetition of uncertain. Figure 8 shows samples No. 2 - 14 from figure 3 by routine double one-dimensional electrophoresis for transferrin. The variants can be clearly identified without difficulties.

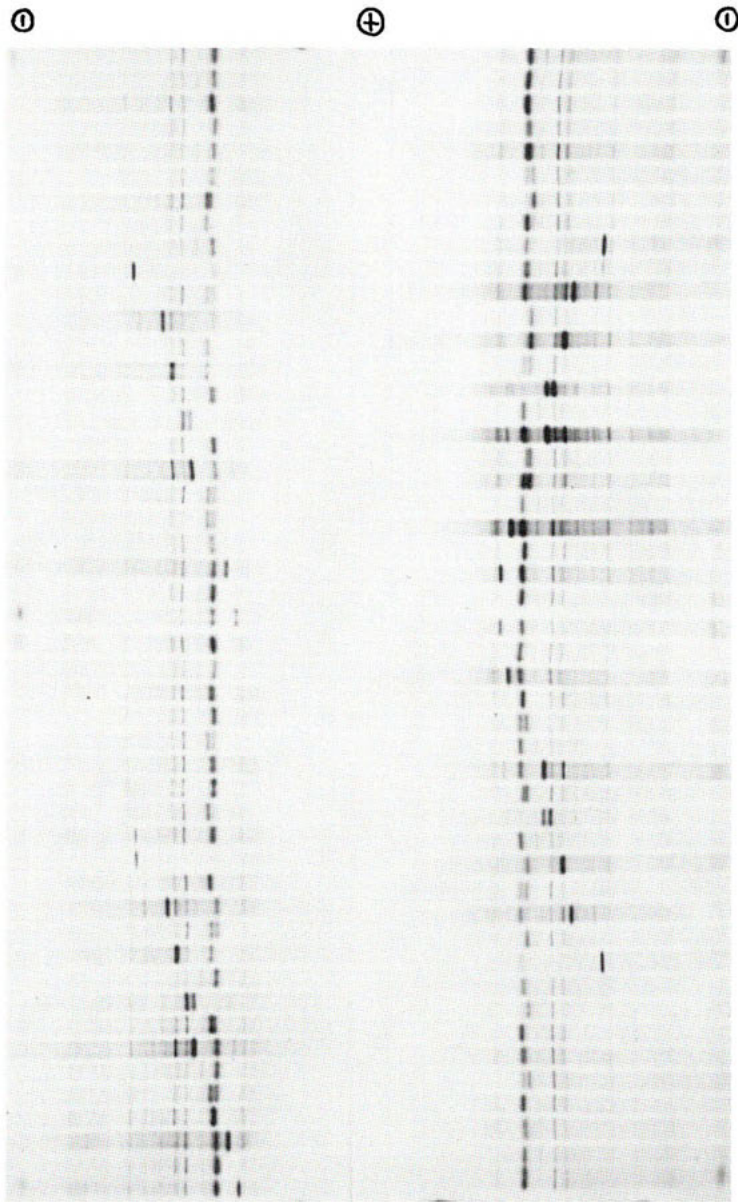


Fig.7: Screening for Tf-variants by double-one-dimensional slab gel electrophoresis. 96 sera (0.25 ul of iron saturated serum is applied) were separated by short distance PAG-electrophoresis and gel strips as indicated in fig. 5 were applied along both cathodic ends of a 4.5 M urea EF-gel (250X190X0.9 mm) with one anode in the middle and two cathodes on both long edges of the gel. Using the electrophoresis system DESAPHOR (DESAGA, Heidelberg) two of these gels or 192 samples can be run simultaneously. Tf-variants are recognized as the most intensive zones in the pattern.

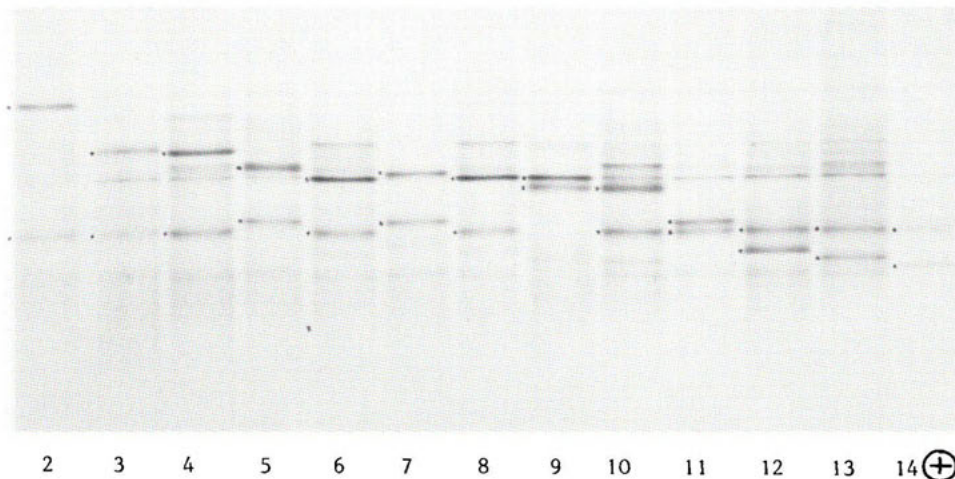


Fig.8: Double-one-dimensional slab gel electrophoresis of iron-saturated transferrins from samples No. 2 - 14 in fig. 3. Samples No. 6 and 8 are identical. After short distance PAG-electrophoresis an unstained gel strip as indicated in fig. 5 (upper gel) was used as sample for subsequent EF. Note that the relative positions of the Tfd-variants are different in the EF- and PAGE-patterns (compare with fig.3d).

The patterns shown in figures 5 and 6 were obtained by short distance PAGE in the first step as shown in figure 5. Figure 9 demonstrates how resolution can be increased to a high level. Comparing the positions of the Tf-compounds in the different samples it appears to be evident that these positions are not occupied by other non-Tf material. This means that optimum resolution has been achieved simply by increasing the migration distance in the first PAGE step and by spreading the pH gradient in the second step. Figure 9 also clearly demonstrates 5 different molecular forms of Fe_2 -Tf which explain the shape of the crossed immunoelectrophoresis pattern in the Fe_2 -Tf region in figure 1 and 10 but were completely hidden by the background in the single step one-dimensional electrofocusing patterns (see figure 1, 2 and 3).

Figure 10 demonstrates another type of double one-dimensional slab-gel electrophoresis. After PAG electrofocusing of many samples the Fe_2 -Tf region has been cut out as a strip and transferred to a gel containing anti-human-Tf-serum. The area of the rockets obtained after electrophoresis corres-

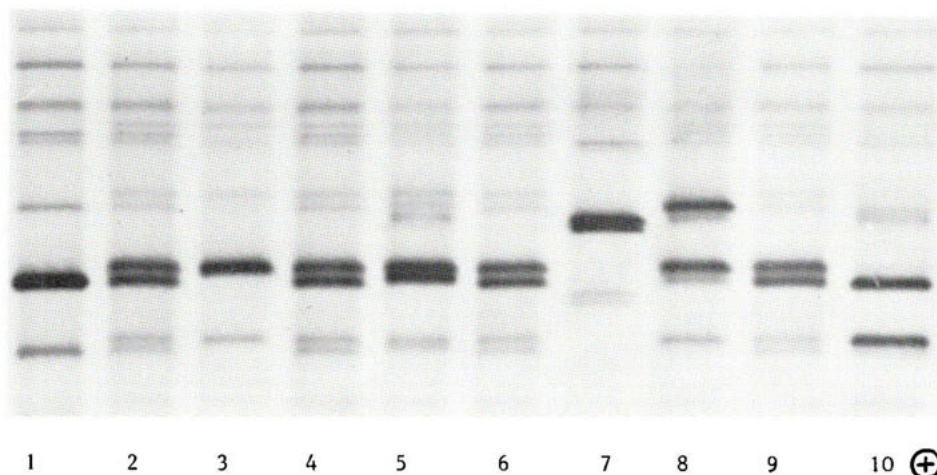


Fig.9: High resolution double-one-dimensional slab-gel electrophoresis of $\text{Fe}_2\text{-Tf}$ from 4 μl serum of different Tf-phenotypes. High resolution was obtained combining long distance PAGE with EF in a spread pH-gradient. Compare the result with that shown in fig. 8. Note that the Tf-patterns are repeated 5 times in all samples with the most intensive in the middle thus explaining the shape of the crossed immunoelectrophoresis pattern in the $\text{Fe}_2\text{-Tf}$ -region (see fig. 1 and 10). Note that only 4 constant non-Tf-zones are seen in the pattern. Such a pattern cannot be demonstrated by single step separation procedures.

ponds with the quantity of $\text{Fe}_2\text{-Tf}$ in the original samples. Wilson et al.(4) described a deficiency of a serum protein in patients with cystic fibrosis focusing at pH 5.48 in 4 M urea gels. Using the technique demonstrated in figure 10 we found that these patients were deficient in $\text{Fe}_2\text{-Tf}$ with an electrofocusing point of pH 5.5 in 4 M urea gels. The protein deficiency in that region thus may be explained as the consequence of a reduced serum iron level in cystic fibrosis patients (5).

Discussion

The two presented examples of double one-dimensional slab-gel electrophoresis provide some interesting aspects of application:

1. It is a very simple procedure: Two established slab-gel techniques are combined by transfer of a strip from one slab to another slab. No spe-

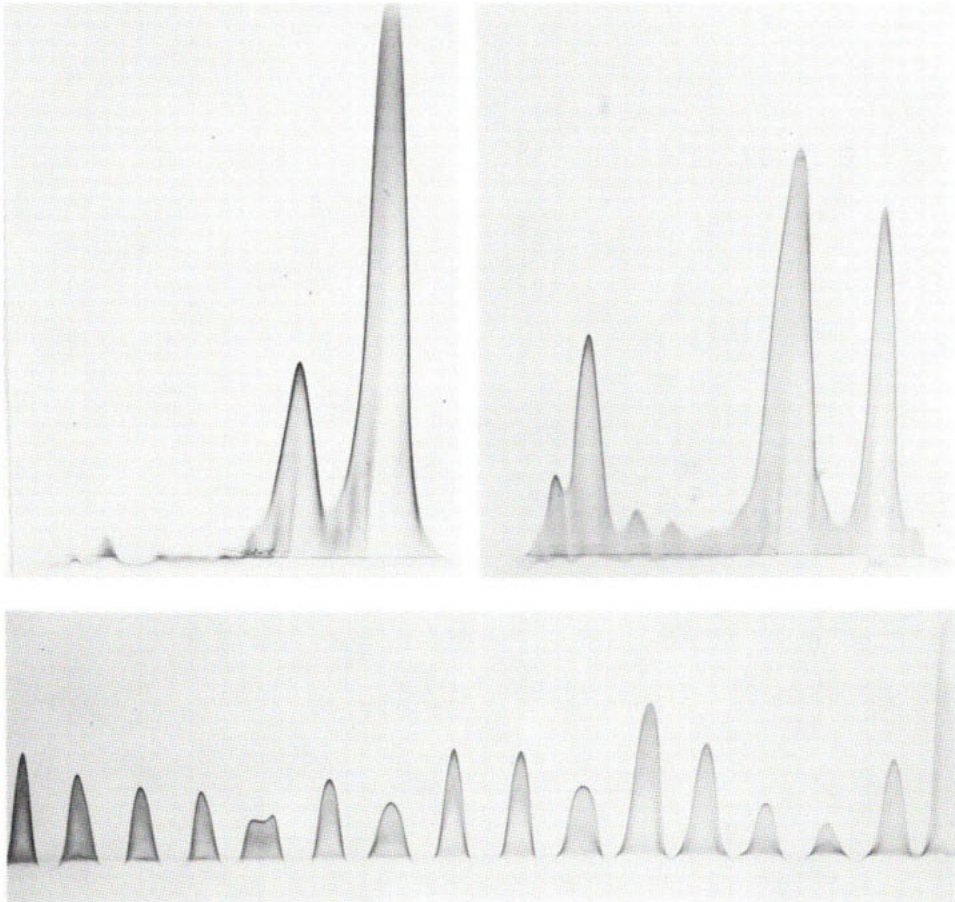


Fig.10: Upper part: Crossed immunoelectrophoresis of Tf from two sera with low (left) and high (right) iron loading (see also figure 1 for explanation). Lower part: Double-one-dimensional immunoelectrophoresis of Fe₂-Tf. After PAG-EF in a slab of many untreated sera the Fe₂-Tf-region (see fig. 2 and 3b)) has been cut out and put on an agarose gel containing anti-human-Tf-serum. The result represents the relative quantity of Fe₂-Tf within the applied set of sera. Obviously Fe₀-Tf and Fe₁-Tf can be quantitated in a similar way.

cial fixation of the strip on the second slab is needed.

2. The sequence and quantity of samples is determined once when they are applied to the first slab-gel system. There is no second source of error in sample sequence and quantity when the second separation procedure is performed.

3. Double one-dimensional electrophoresis is a method to provide optimum resolution of areas of interest in single step one-dimensional electropherograms. The slab-gel technique provides the special advantage of multiple sample treatment.
4. Double one-dimensional slab-gel electrophoresis in the sequence PAGE—PAG electrofocusing has the special advantage that the last separation step is that with the highest resolution. Thus the resolution of this technique is expected to be even higher than that of the high resolution two-dimensional techniques where the electrofocusing step is always applied first. This argument appears to be especially valid when genetically determined position variants due to charge are concerned.
5. Interindividual comparison of a reduced number of compounds from many individuals at the level of optimum resolution may be performed simply by inspection with regard to quality and by standard densitometry with regard to quantity. There is no sophisticated equipment necessary.
6. The fact that optimum resolution can be obtained by this method provides the possibility for the comparative study of compounds for which specific staining procedures including immunofixation are not available or accompanied by loss of resolution due to diffusion during the incubation.
7. The technique demonstrated in figure 10 provides the possibility for the multiple selective quantitative estimation of biochemically different but immunologically identical antigens as the different molecular forms of transferrin in this case.

Besides the two presented examples of double one-dimensional slab-gel electrophoresis there are many other interesting combinations possible. One is to start with electrofocusing in PAG or agarose and to continue with a molecular sieve electrophoresis. Another would be to concentrate diluted samples and separate in the first step by displacement electrophoresis in the presence of proper ampholytes and to continue with a molecular sieve electrophoresis, with electrofocusing or an immunological procedure.

Double one-dimensional slab-gel electrophoresis provides a broad field of

variation and application. There is no limitation to go to a triple one-dimensional system if necessary. With regard to special aspects the method provides advantages over single step one-dimensional and two-dimensional procedures. There are certainly other aspects where single step one-dimensional or two-dimensional techniques have advantages over double one-dimensional procedures. It depends on the aspect which procedure is best.

References

1. Altland, K., Schmidt, S. R., Kaiser, G., Knoche, W.: Demonstration of a Factor in the Serum of Homozygotes and Heterozygotes for Cystic Fibrosis by a Non-Biological Technique. *Human Genetics* 28, 207 (1975)
2. Altland, K., Hackler, R., Knoche, W.: Double One-Dimensional Electrophoresis of Human Serum Transferrin: A New High Resolution Screening Method for Genetically Determined Variation. *Human Genetics* (in press)
3. Altland, K., Hackler, R., Knoche, W., Greiner, J., Benckmann, H. G., Goedde, H. W.: Demonstration of New Transferrin Variants in Different Populations. *Human Genetics* (in press)
4. Wilson, G. B., Jahn, Th. L., Fonseca, J. R.: Demonstration of Serum Protein Differences in Cystic Fibrosis by Isoelectric Focusing in Thin-Layer Polyacrylamide Gels. *Clin. Chim. Acta* 49, 79 (1973)
5. Altland, K., Hackler, R., Knoche, W.: Serum Iron Deficiency in Cystic Fibrosis Patients as a Source of Changes of the Electrofocusing Pattern of Serum Proteins (in preparation)

ULTRATHIN-LAYER HORIZONTAL ELECTROPHORESIS, ISOELECTRIC FOCUSING, AND PROTEIN MAPPING IN POLYACRYLAMIDE GELS ON CELLOPHANE

A. Görg, W. Postel, and R. Westermeier

Lehrstuhl für Allgemeine Lebensmitteltechnologie der Technischen Universität München, 8050 Freising-Weihenstephan, FRG.

Abstract

Methods of ultrathin-layer horizontal electrophoresis, isoelectric focusing, and protein mapping as a combination of these two techniques in 0.12, 0.24, respectively 0.36 mm polyacrylamide layers on a foil are described. The advantages of these ultrathin-layer techniques in handling, resolution, time, and cost, compared with the conventional methods in 1 - 2 mm thick polyacrylamide layers, are demonstrated. A few application examples are presented.

Introduction

Thin-layer isoelectric focusing, described a decade ago (1,2), was adopted with only minor modifications in a great number of subsequent publications. While in some early contributions 1.5 - 3 mm thick gel layers were used (3-5), in an increasing number of recent publications 1 mm gel layers were preferred. In 1975 precast polyacrylamide gels (LKB PAG-Plates) appeared on the market. The thickness of the gel layer was 1 mm too; the new fact, however, was that those polyacrylamide gels adhered to a plastic foil, resulting in great advantages compared with thin-layer gels polymerized on glass plates (6). Because these precast gels adhere firmly to the foil during the

focusing procedure as well as the visualization operations applied for protein and enzyme staining they are superior in handling to conventional gels polymerized on glass plates. We considered the mechanical stability of those precast gels so attractive, that we did not want to work with gels polymerized on glass plates any longer. For financial reasons, however, we were obliged to prepare our polyacrylamide gels on foils ourselves.

We reported on the laboratory preparation of polyacrylamide gels on cellophane supports in 1977 (7). Here, we have not only succeeded in cutting costs considerably - compared with precast gels -, but also in preparing foil-supported polyacrylamide gels of different sizes, different C and T values, pH-gradient regions as well as with or without additives (sucrose, glycerol, urea, SDS etc.). The gels adhere firmly to the cellophane, can be handled conveniently, are protected from fracture during all the steps of the operation, keep their original size, and can be easily dried for documentation.

The mechanical stability of these gels polymerized on cellophane has enabled us to take a step forward, reducing the thickness of the gel layer from 1 mm - which was so far considered to be the minimum - to nearly a tenth of this. The preparation of these ultrathin-layer gels was described in 1978 (8,9). In this way, the advantages of ultrathin-layer gels, expected in theory (6,10,11), could be put into practice for the first time:

As a result of the reduced gel layer thickness, the improved cooling effect makes it possible to apply higher field strength to achieve improved resolution and shorter separation time. Protein staining and destaining as well as zymogram methods run particularly fast in comparison with conventional gels. Finally, gel layers of reduced thickness are attractive from the point of cost analysis by decreasing the demand for carrier ampholytes, which are still considered a limiting

factor for some applications.

As we have determined in further experiments, ultrathin polyacrylamide gels on cellophane supports are not only advantageous for isoelectric focusing, but also for electrophoresis and protein mapping. The basis for ultrathin-layer electrophoresis, isoelectric focusing, and protein mapping is the ultrathin polyacrylamide gel on a sheet of cellophane (8,12,13), which can always be prepared on the same principle with only simple modifications, as follows.

Material and Methods

The polymerization of the ultrathin gels is performed in a glass polymerization chamber (LKB's system). One of the two glass plates is covered with cellophane, and instead of the conventional rubber gaskets parafilm is used. The simplicity of these two materials - both are common foils; parafilm in the laboratory, cellophane in the household for the closing of jam jars - should enable every laboratory to prepare ultrathin-layer polyacrylamide gels on foils without any particular effort.

- 1) Preparation of ultrathin polyacrylamide gel layers. Ultrathin gel layers can be polymerized from conventional stock solutions for electrophoresis or isoelectric focusing, chemical or photochemical, with or without additives (as for example sucrose, urea, glycerol, starch etc.). The polymerization chamber is built up as follows (8,9,15): A sheet of cellophane is soaked with distilled water and carefully mounted on a glass plate. The drying cellophane then straightens itself on the glass plate. The gel thickness can be varied by choosing the suitable number of parafilm layers (one layer corresponds to 0.12 mm, two to 0.24 mm etc.). For the preparation of ultrathin gel layers

for horizontal electrophoresis or protein mapping, the top glass plate is replaced by a slotformer (12) or a mould, respectively, both of which we made ourselves (fig. 1). The moulded gel troughs are intended for the insertion of the strips cut from the gel with the previously focused proteins. Corresponding protein samples are pipetted into the slots for simultaneous runs.

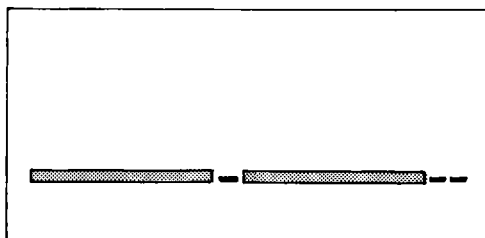


Fig. 1:

Mould for gel casting for ultrathin-layer horizontal electrophoresis as the second dimension of protein mapping. Parafilm strips and pieces stuck on a glass plate with an adhesive of two constituents.

Two smooth spatulas or paper clips as spacers are wedged between the upper edges of the two glass plates. The calculated volume of the deaerated polymerization solution is poured into the chamber (to about half of the height) by a syringe with a blunt needle. When the spatulas or the paper clips are removed and the clamps at the lateral edges are replaced, the liquid level rises to the upper edge (8). It is not necessary to cover the gel solution with water. After completed polymerization, the gel in the polymerization chamber (without clamps) is cooled in a refrigerator and can be stored there until use.

- 2) Separation run. The top glass plate, the slotformer or the mould, respectively, is removed by carefully twisting a smooth spatula or a small knife between the glass plates. The gel prefers to adhere to the cellophane rather than to the glass plate. The parafilm gasket is removed and can be used several times. The ultrathin gel on cellophane is carefully mounted on the cooling block of the multiphor chamber, which had previously been wetted with a small

quantity of kerosene for good contact and heat transfer.

Isoelectric focusing is performed in the conventional manner (8,13). Because of the improved cooling efficiency, higher field strength can be applied, resulting in shorter focusing time.

We performed the ultrathin-layer horizontal *electrophoresis* (13) according to the publication of FEHRNSTRÖM and MOBERG (14) in a tris-glycine buffer system with pH=8.9 at 10 °C. After 10 min preelectrophoresis with a preset constant current of 15 mA, sample solutions are pipetted into the slots. The proteins are concentrated by the gel edges of the slots while they penetrate the separation gel with a current of 7 mA for 10 min. The separation is run with a preset constant voltage of 200 V. For the detection of the migration front a small volume of bromphenol blue is added to each sample.

In *protein mapping* gel strips containing focused proteins are cut from the ultrathin focusing gel with a razor blade to a suitable size for the gel troughs. With the aid of two pairs of tweezers these gel strips are laid into the troughs for electrophoresis, cellophane support uppermost. Air bubbles are smoothed out. Polymerization of the gel strips into the troughs is not necessary. In order to achieve concentrating effect at the trough edges, a higher acrylamide concentration has to be chosen for the electrophoresis gel than for the focusing gel. In our experiments, shown here, we used gel layers with 5 % T for focusing and 7.5 % T for electrophoresis.

- 3) Staining. Any conventional protein and enzyme staining techniques can be applied. With decreasing thickness of the gels substantially shorter times for the operations are obtained, as shown in table 1.

Table 1: Comparison of the Times for Staining and Destaining of Conventional and Ultrathin-Layer Gel Slabs

Gel thickness (mm)	Fixation with TCA (min)	Staining with 0.1 % coomassie blue G-250 (min)	Destaining (hr)	Total time (hr)
1	120	45	24	27
0.24	30	20	2	3
0.12	10	5	1/4	1/2

Particularly sharp enzyme bands are obtained (for instance in polyphenoloxidase staining technique), if the ultrathin gel is dipped into the substrate solution for a few minutes and dried at once with the aid of a hair dryer. Enzyme bands develop during the drying procedure without diffusion.

It is suggested that gels for glycoprotein staining should be polymerized on a "Mylar" polyester foil, for cellophane does not react neutrally during glycoprotein staining techniques. The method for the preparation of ultrathin gels on polyester foils was reported by us in early 1979 (12,15).

- 4) Drying and storage. The stained ultrathin gel is mounted on a plexi-glass plate after brief impregnation in a solution of glycerol-water-methanol (3:27:70 v/v) (16). The superfluous cellophane along the long side is folded to the underneath. The edges along the short side are fixed with self-adhesive tape (13). The gel can be dried either in air, in an oven, or within a few minutes with the aid of a hot fan. A cover foil is not necessary. The transparent pherograms can be photographed, evaluated by densitometry, and stored for documentation without change. It is also possible to transfer the ultrathin gel from the cellophane to a sheet of paper.

In the protein mapping technique, simultaneously stained gel